REPUBLIC OF TÜRKİYE

ALTINBAŞ UNIVERSITY

Institute of Graduate Studies

Electrical and Computer Engineering

A NOVEL MINIATURIED RADAR ANTENNA DESIGN IN KU BAND FOR V2X COMMUNICATION

Saif Al-deen Kamal HEYAD

Master's Thesis

Supervisor

Assoc. Prof. Dr. Doğu Çağdaş ATİLLA

Istanbul, 2023

A NOVEL MINIATURIED RADAR ANTENNA DESIGN IN KU BAND FOR V2X COMMUNICATION

Saif Al-deen Kamal HEYAD

Electrical and Computer Engineering

Master's Thesis

ALTINBAŞ UNIVERSITY

2023

The thesis titled A NOVEL MINIATURIED RADAR ANTENNA DESIGN IN KU BAND FOR V2X COMMUNICATION prepared by SAIF AL-DEEN KAMAL HEYAD and submitted on 03/03/2023 has been **accepted unanimously** for the degree of Master of Science in Electrical and Computer Engineering.

_____

Assoc. Prof. Dr. Doğu Çağdaş ATİLLA
Supervisor

Thesis Defense Committee Members:

Assoc. Prof. Dr. Doğu Çağdaş ATİLLA	Department of Electrical and Electronics Engineering, Altınbaş University	_____
Asst. Prof. Dr. Muhammad IL YAS	Department of Computer Engineering, Altınbaş University	_____
Asst. Prof. Dr. Cahit KARAKUŞ	Department of Computer Engineering, Esenyurt Univrsity	_____

I hereby declare that this thesis/dissertation meets all format and submission requirements of a Master's thesis.

Submission date of the thesis to Institute of Graduate Studies: ___/___/___

I hereby declare that all information/data presented in this graduation project has been obtained in full accordance with academic rules, and ethical conduct. I also declare all unoriginal materials and conclusions have been cited in the text and all references mentioned in the Reference List have been cited in the text and vice versa as required by the abovementioned rules and conduct.

Saif Al-deen HEYAD

Signature

DEDICATION

This thesis was completed while I was pursuing my Master's degree in electrical and computer engineering at Altnbaş University.

First, I'd want to express my gratitude to Assoc. Prof. Dr. Doğu Çağdaş ATİLLA, my supervisor, for giving me the chance to join his research group and learn more about this exciting and modern field of research. As I did the research and wrote up this thesis, Dr. ATİLLA gave me helpful feedback and advice.

I'd also want to thank Eng. Faruq KURTULUS, the research assistant and lab coordinator, for all his assistance with antenna production.

Lastly, but certainly not least, I am grateful to my parents and brothers for their unwavering support throughout the entirety of my graduate studies. You made everything possible.

ABSTRACT

A NOVEL MINIATURIED RADAR ANTENNA DESIGN IN KU BAND FOR V2X COMMUNICATION

HEYAD, Saif Al-deen

M.Sc., Electrical and Computer Engineering, Altınbaş University,

Supervisor: Assoc. Prof. Dr. Doğu Çağdaş ATİLLA

Date: April / 2023

Pages: 64

The thesis introduces a novel, compact, miniaturized, and low-cost antennas. The proposed antenna designed on Rogers RT5880LZ lossy and simulate by CST microwave studio. Novel single element antenna design resulted in a new slotted circular microstrip antenna, which produced two high directive, gain, and low sidelob level array antennas for Ku band V2X radar.

The measured S11 for single element, 1x4 and 3x4 antenna array was –24.5 dB, –39.47 dB and –32.16 dB respectively. Moreover, 3x4 antenna design with 12 element have obtain the highest gain of 16.3 dBi with minimum SLL –30 dB in both of E-plane / H-plane.

Keywords: Microstrip Antenna Array, Automotive Radar, Ku-Band Application, Sidelobe Level, Reflection Coefficient (S11), Series Feed, And Gain.

TABLE OF CONTENTS

Pages

LIST OF TABLES

Pages

LIST OF FIGURES

Pages

ABBREVIATIONS

V2X : Vehicle to Everything

V2V : Vehicle to Vehicle

V2S : Vehicle to Satellite

ITS : Intelligent Transportation Systems

AI : Artificial Intelligence

SAE : Society of Automotive Engineers

LRR : Long-Range-Radars

MRR : Mid-Range-Radars

SRR : Short-Range-Radars

BW : Band width

MPA : Microstrip Patch Antenna

SLL : Sidelobe level

LIST OF SYMBOLS

μ : Electron-Mobility.

λ : Wavelength.

ω : Angular-Frequency

ε_r : Dielectric Permittivity

θ : Theta

φ : Phi

Γ : Reflection Coefficient

H : Magnetic Field Intensity

λ_0 : Free Space Wavelength

$tan\delta$: Loss Tangent of the Substrate

1. INTRODUCTION

1.1 TECHNOLOGIES EVOLUTION

Currently, and because of the evolution of radio communications technologies for Intelligent Transportation Systems (ITS) over the past decade, the car is intelligent. Increasingly autonomous cars are enabled by a variety of technology around the vehicles, including artificial intelligence (AI), image processing, and numerous and sophisticated sensors. There are a growing number of applications for automotive radar systems in automobiles around the globe. These components are used in sophisticated Automotive vehicle systems. It is projected that the usage of these systems will become more frequent within the foreseeable future, particularly the civilian use of Ku band and mm wave radars for navigation, road traffic management, safety for highway driving, and security purposes in addition, satellite antenna and V2S antenna while the ku band have been chosen [1], [2].
In the near future, autonomous vehicles will be both safe and efficient. While automakers and tech companies around the world promote the concept of self-driving cars, advanced driver assistance systems are advancing rapidly. lane change assist, Adaptive cruise control and enhanced emergency braking are examples of technology that are not exclusive to luxury vehicles. ADAS, This is equivalent to or lower than level 2 according to the Society of Automotive Engineers (SAE) criteria Autonomous Vehicle Technology, can be viewed as the foundational technology for advancing to greater levels of automation [3]. Typically, a variety of sensors, such as camera, radar, and lidar, are incorporated into these systems. Specifically, radar sensors play an important function because to their resistance to extreme weather conditions [4]. Radar sensors in automobiles can identify the distance, angular position and velocity of nearby targets. Current market radar sensors are typically categorized according to their function as long-range-radars (LRR), mid-range-radars (MRR) [6], and short-range radars (SRR). LRRs commonly have a narrow beam, can monitor distances up to 200 meters, and utilized in adaptive cruise controls. While in the short range radar the bandwidth is wider where gives a better image resolution and typically required in parking function [4].
To meet the future demands of fully automated and autonomous driving, the performance of car radar sensors must be enhanced. To accurately determine, for instance, the shape and direction of the surrounding cars, higher-resolution radar images are required [5]. The

radar sensor is not going to function properly without the antenna system. Planar antenna arrays, which are often microstrip arrays, are now the most popular option for achieving both cheap production costs and compact sensor dimensions. This is made possible by the utilization of planar antenna arrays. However, microstrip antennas have a limited frequency range [7].

1.2 RESEARCH MOTIVATIONS

As the need for automotive radar antennas is high because technology is changing and V2X communication is about to be used, this work focused on designing microstrip array antennas that work at ku band frequencies and have a small form factor to meet the size limit, high radiation efficiency, relatively high gain, and low side lob level. In this thesis, a proposal is made for the creation of microstrip patch antennas in array format so that they can be utilized for Ku band applications.

As this frequency band has multiple applications based on the characteristics of antenna design, the (V2V) Automotive radar and satellite antenna might share the majority of their specifications. The architecture is compatible with both radar and fixed satellite or direct vehicle-to-satellite broadcasting (V2S). In addition, numerous antenna characteristics linked to total radiation performance, such as antenna kind, feeding mechanism, substrate selection with respect to dielectric constant, thickness, loss tangent, etc., were investigated. As a result of this research, a wideband series feed design guide for Ku band antenna array applications has been developed.

1.3 RESEARCH OBJECTIVES

This dissertation focuses on Method for developing and implementing of a new single element microstrip antenna design to array antenna for automotive radar and Ku band applications, which provides the reliability required for effective integration in a vehicle and is capable of coping with the increased BW resolution potential offered by a single layer and low dielectric constant. In particular, to attain these objectives, the following are the key contributions of this thesis:

First, Small size is a crucial factor in automotive radar. To avoid the challenges associated with radar-vehicle integration, certain automobile models expose the radar through an opening in the grille. however, printed antenna array with small size would be suitable for

this purpose. high frequency in mm-wave bands can be smaller, but in the other hand, the fabrication and cost in ku band better and easier.

Second, bandwidth and directivity. Most of the wideband antennas are attainable by using high dielectric constant and thicker substrate design. However, the main lobe direction degree cannot be controlled affected by the loss tangent. In the other hand, using low dielectric and thin substrate will limit the bandwidth which is the factor of represent the resolution in Radar and the throughput in satellite application. Nevertheless, thin substrate and low dielectric can provide appropriate BW with maintaining the directivity.

1.4 THESIS OUTLINES

This thesis' structure is composed of five chapters. The first one is an introduction of technology evaluation Background, goals, research motivation and scope of the project, as well as a summary of the thesis, are presented in the first chapter.

The second chapter serves as a state-of-the-art analysis, providing a survey of antenna theory and description the state of the art in antenna technology for radar and ku band application Key antenna performance factors, such as radiation efficiency, gain and bandwidth, are described in this chapter as well.

In the third chapter, we will discuss the process of creating radiation elements. The work involves parametric research to select the optimal design for a 14.4 GHz as center frequency antenna based on a circular single patch antenna as the radiation element.

Furthermore, in forth chapter, the substrate and feeding method are discussed briefly for the array design. In order to assess the far-field behavior for the proposed antenna array, CST microwave studio simulations were run on a circular array.

The suggested antennas were Fabricated and tested in Chapter 5, with results that were in line with expectations.

Chapter 6's conclusion and discussion of potential future work for Automotive and V2X future for Ku band.

2. STATE OF ART

2.1 INTTODUCTION TO ANTENNAS

Radar can't function without its antenna array. Since the array performance has such a large impact on the radar's capacity to accurately detect targets, it is crucial to set some specifications and criterion for evaluation that may precisely characterize the connection between radar performance and array designs [8]. as known, main purpose of the antennas is to receive and transmitting the electromagnetic-waves. By collecting and converting the radiated electromagnetic-waves in free space to guided-waves contained by transmission line, waveguide or feeder cable as receiving component [9]. And vis versa as a radiating component as shown in Figure 1.1 [9]. In radar the Same mechanism of the antenna but the receiving waves represent the reflection of the transmitted ones. Therefore, the message here is an image of the reflector or the target [8]. It is worth mentioning here if the purpose is to obtain the reflection of the target, what is the benefit of bandwidth. Simply here, the bandwidth expresses the accuracy, or we can say that each single frequency represents a pixel in the reflected image, so the bandwidth is a great importance in improving image resolution.

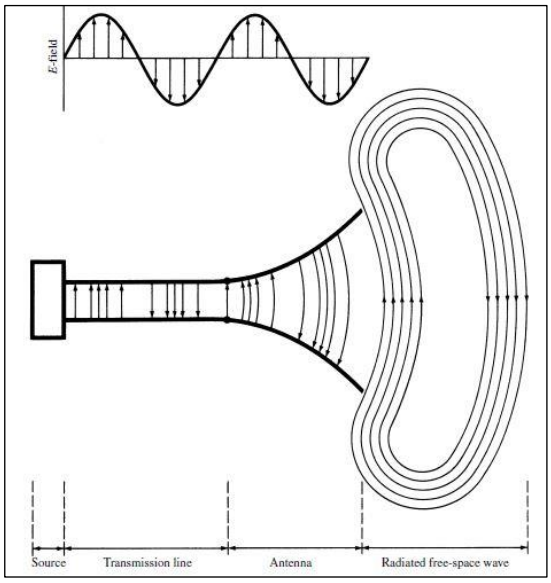

Figure 2.1: Antenna Mechanism Work [9].

As depicted in Figure 1.2, the antenna could be represented in transmission line form using electrical equivalent circuit. It is not desired that there be losses on account of the

line, the antenna, and standing waves. Selecting low-loss lines is one way to cut down on transmission losses while decreasing the loss resistance expressed by RL is one way to cut down on antenna losses. The line's energy storage capacity should be decreased and standing-waves minimized. through adjusting antenna (load) impedance to be compatible with the line's characteristic impedance. In this case, the antenna stands in for the load that must be matched to the transmission lines [9]. When the antenna is utilized in its receiving configuration, the source is swapped out for a receiver, and a diagram resembling Figure 1.2 is used to depict the system. All other parts comparable components remain unchanged. In the receiving mode, the radiation-resistance Rr represents the transmission of energy again from free-space wave to the antenna.

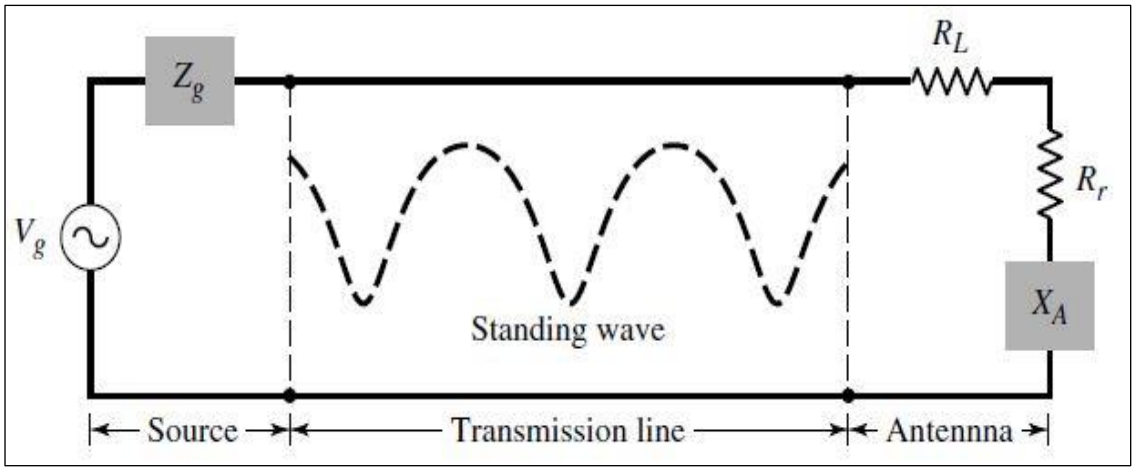

Figure 2.2: Thevenin Equivalent Circuit to Antenna As A Transmission Device [9].

An antenna in a state-of-the-art wireless system not only receives or transmits energy but also optimizes or magnifies the radiation energy in specific directions while suppressing it in others. Therefore, in addition to acting as a probe, the antenna needs to provide direction. Depending on the application, where the radar and satellite antennas are needed for the directive application. antenna may take the form of an aperture, a patch, an array, conducting wire, a lens, a reflector, or any other form that meets the requirements.

According to Maxwell's equations, any time-varying magnetic or electric field that has an orthogonal orientation will produce the opposite field and will result in the formation of an electromagnetic wave. Table 2.1 contains a presentation of the rules of electromagnetism that were formulated by Maxwell as:

The initial equation used to anticipate changes in electric fields, where D is the electric flux density and ρv is the volume change density.

The second one for predict electric fields changes, where B represent the magnetic flux densities.

The third and fourth formulas provide for the propagation of electromagnetic waves by inducing current displacement and generating a magnetic field, which in turn generates an electric field. Where Electric/magnetic field intensity are denoted by E and H, respectively and J is the electric current density.

Table 2.1: Maxwell Equations [10].

Differential Form	Integral Forms	Description
$\nabla \cdot D = \rho_v$	$\oint \boldsymbol{D}.d\boldsymbol{S} = \oint \rho_v \,.dv$	Gauss's law
$\nabla \cdot B = 0$	$\oint \boldsymbol{B}.d\boldsymbol{S} = 0$	magnetic charge "Nonexistence of isolated"
$\nabla \times E = -\frac{\partial B}{\partial t}$	$\oint E.d\boldsymbol{L} = -\frac{\partial}{\partial t}\int B.d\boldsymbol{S}$	Faraday's Law
$\nabla \times H = J + \frac{\partial D}{\partial t}$	$\oint H.d\boldsymbol{L} = \int (J + \frac{\partial D}{\partial t}).d\boldsymbol{S}$	Ampere's Law

2.2 ANTENNA KEY PARAMETERS

2.2.1 Antenna Radiation Pattern

The antenna radiation pattern, also known as an antenna pattern, is defined as "a mathematical function or a graphical explanation the radiation qualities of the antenna as a function of spatial coordinates." An antenna pattern is also known as an antenna radiation pattern. radiation pattern is typically established in the far-field area and is characterized as a function in directional coordinates. This is because the far-field region is the most unobstructed part of the electromagnetic spectrum [10]. Lobes are used to refer to the various portions of a radiation pattern, and they can be further subdivided into main as (major), secondary as (minor), side, and rear lobes. Lobes can also be called segments. A "part of radiation pattern bordered by regions of comparatively weak radiation intensity" is what we mean when we talk about a "radiation lobe." The illustration in Figure 2.3a depicts 3-dimensional symmetrical polar pattern that has a number of radiation lobes. Although some lobes have a higher radiation intensity than others, they are all still considered to be lobes. Figure 2.3b depicts a linear 2-dimensional design for reference.

In this pattern and following ones, the proportional polarization of the amplitude between the multiple lobes is shown by minus (-) and plus (+) signs that appear in the lobes. This relative polarization shifts (alternates) whenever the nulls are crossed. the highest value of the pattern may be observed from the -3 dB or 0.707 from the maximum main lobe, which was explained in 2.3a to indicate the Half Power Beam width (HPBW). one of most important considerations that go into choosing an antenna for a certain application is the radiation pattern, which can take on a variety forms, including the main ones listed below [10]:

a. Isotropic
b. Directional
c. Omnidirectional

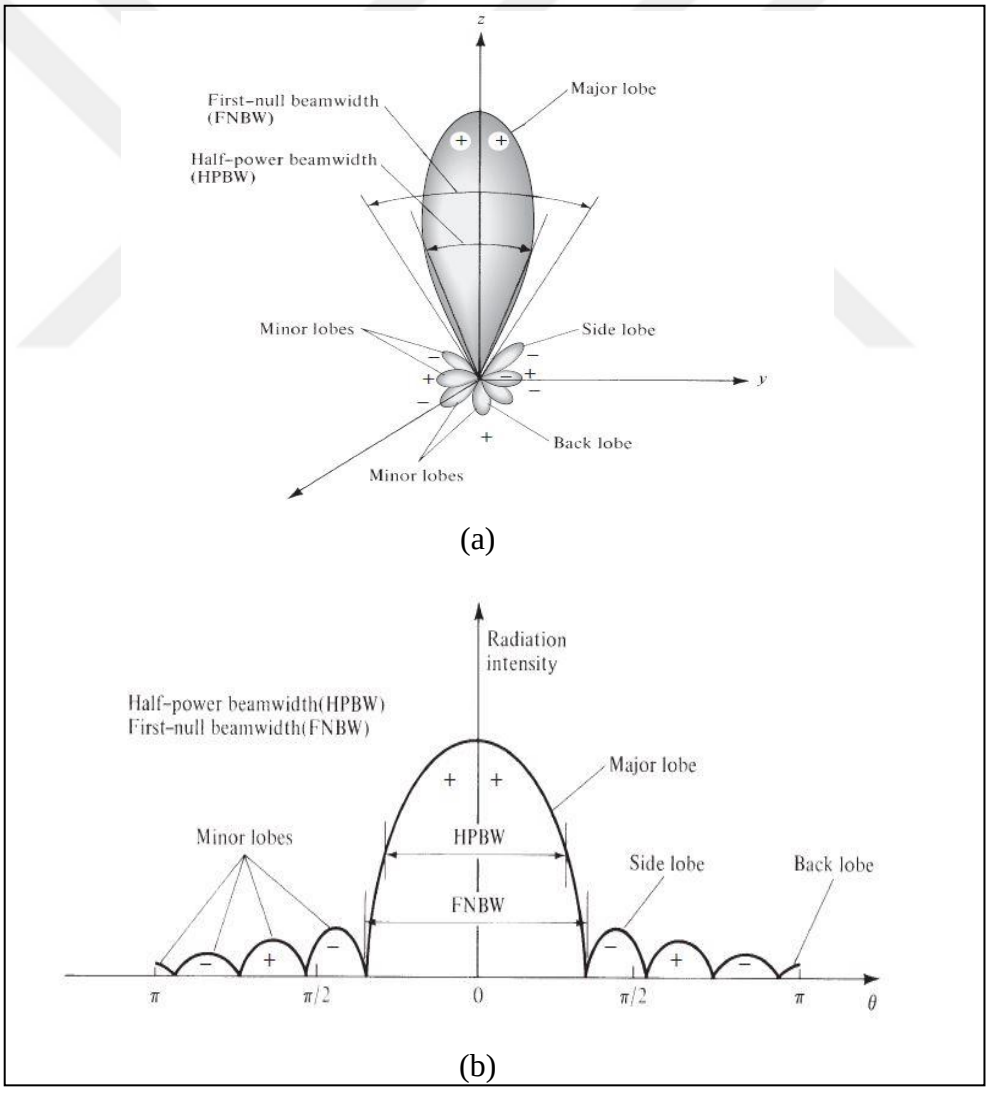

Figure 2.3: (A) 3D-Directional Radiation Pattern, (B) Linear 2D Radiation Pattern [10].

Isotropic radiator can explain "a hypothetical lossless antenna with equal radiation in all directions," according to the definition of the term. Even though it is a theoretical construct and cannot be realized in practice, it is frequently used as a point of reference for measuring the directional features of real antennas.

The omnidirectional radiation has the property of being non-directional in the plane of azimuth ($\theta = \pi/2$) but directional in the plane of elevation (φ =constant), as can be seen in Figure 2.4 [10].

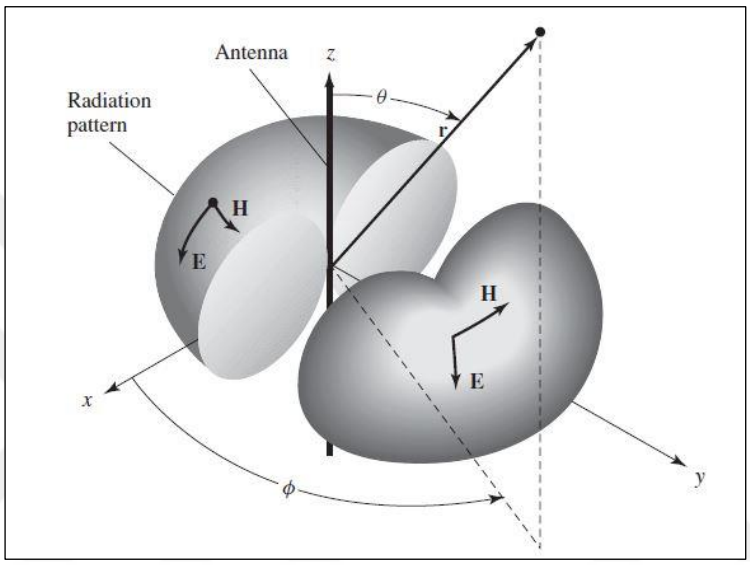

Figure 2.4: Omnidirectional Pattern [10].

The definition of what is known as “directional antennas” are having the property of emitting or receiving electromagnetic radiation more successfully in certain directions more than others as shown in Figure 2.3a. Because of the importance of directionality to both radar and satellite technology, this task requires the employment of directional fields in both of those technologies. When using radar for a directed application, the primary lobe should get the greatest amount of power, while the power delivered to the other lobe's sides and back should be reduced.

It is common practice to discuss the performance of a linearly polarized antenna in terms of E-plane pattern and H-plane pattern of the antenna.

a. The E-plane is the plane that has been determined to contain both the vector of the electric field and the direction in which the largest amount of radiation is emitted.
b. The H-plane that is characterized by the fact that it contains both the vector of the magnetic field with maximum radiation direction.

2.2.2 Gain And Directivity

Gain of the antenna (in a specific direction) is described as "the ratio of the intensity in a particular direction to the electromagnetic intensity that could be gained if the antenna absorbed power and radiated it isotropically with the same amount of input power. the gain with a lossless isotropic reference antenna source in the following equation [9][10] :

$$G = \frac{4\pi U(\theta,\varphi)}{Pin(losslessisotropicsource)} (\text{dimensionless} \quad (2.1)$$

The antenna-directivity can defined as "the ratio of the intensity radiation in a given angle from the antenna to the average radiation intensity in all directions." As expressed in the Equation:

$$D = \frac{U}{U_o} = \frac{4\pi U}{P_{rad}} \quad (2.2)$$

Where?

G: Gain (dimensionless).

D: directivity (dimensionless).

U: radiation intensity W/unit (solid angle).

U_o: isotropic source radiation intensity W/unit (solid angle).

P_{in}: Total input power (W).

P_{rad}: total radiated power (W).

2.2.3 Efficiency

The efficiency of radiating element defined as the ratio of output power to the input power. a number of antenna efficiencies are connected and can defined by using Figure 2.5 [9]. According to the explanation, there are losses that can reduce efficiency. The first and most significant is the mismatch reflection between the impedance of the input terminals and the impedance of the radiated element. This Factor is the reflection coefficient.

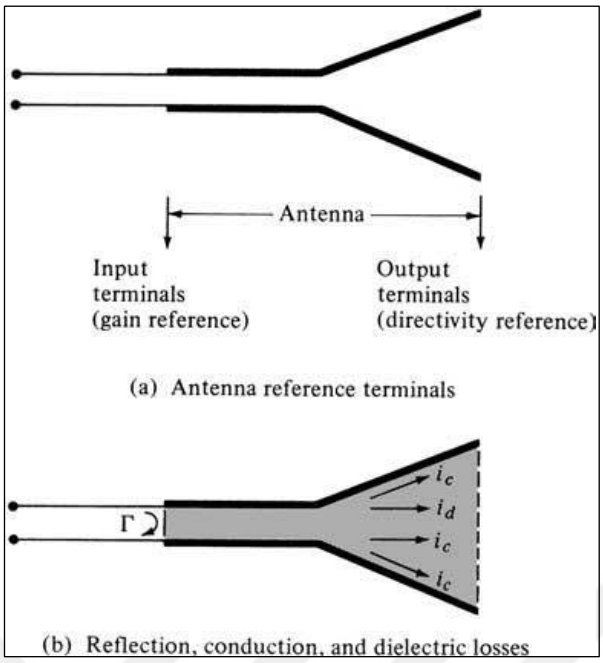

Figure 2.5: Losses And Reference Terminal Of The Antenna [9].

when the mismatch causes a portion of the input power to be reflected. In addition to conduction and dielectric losses, total efficiency is defined as follows:

$$E_o = E_r E_C E_d \tag{2.3}$$

Where?

E_o : Total-efficiency.

E_r : a Mismatch reflection efficiency = $(1 - |\Gamma|^2)$.

E_c : conduction-efficiency.

E_d : dielectric-efficiency.

Γ: reflection-coefficient at the input terminal of the antenna.

2.2.4 Bandwidth

Bandwidth defined as "the range of frequencies over which the performance of an antenna adheres to a particular standard with regard to some feature. The bandwidth can be thought of as the range of frequencies surrounding the central frequency. The necessity of communication bandwidth for data transfer and channel capacity [10]. However, in radar, the bandwidth represents the detecting target's resolution. Every frequency in this miner corresponds to a pixel in the reflected image [8]. In contrast to other radars whose job is to

identify the target's shape, the primary function of automotive radar is detection rather than identifying the target's shape. In this work, we increase the bandwidth of automotive radar to make it acceptable for both radar and satellite applications.

The impediment Bandwidth denotes the bandwidth over which the antenna and its transmission-feed line are matched. In this regard, input incident energy losses due to reflection is less than 10%. At its input terminal, the impedance produced by the antenna varies with frequency. If this impedance does not equal that of the antenna, the impedance mismatch occurs, and the maximum transmission of power is not possible. When measuring impedance bandwidth, it is necessary to characterize both the Reflection Coefficient (S11) and 'voltage standing wave ratio' (VSWR) across the whole band of interest.

Reflection Coefficient:

The reflection coefficient, denoted by the Γ, and described as the ratio of the wave that is reflected to the wave that is incident in (2.4).

$$\Gamma = \frac{Z_{in} - Z_0}{Z_{in} + Z_0} \tag{2.4}$$

Where?

Z_{in}: Input antenna impedance.

Z_0: Transmission line characteristic impedance.

RL Return Loss:

RL is a measurement that indicates the difference here between power that is input into a transmission circuit and the power that is reflected off at the terminal antenna. In many cases, it is expressed as the ratio in decibels. It is possible to describe it as:

$$RL = -20\log10|\Gamma| \tag{2.5}$$

$$RL(dB) = 10\log10\left(\frac{P_{in}}{P_{reff}}\right) = -10\log|S11|^2 \tag{2.6}$$

Where?

P_{in} : incident power.

P_{reff} : reflected power to the source.

The frequency range, on each side of centre frequency of the antenna resonant, where the properties of the antenna are all within an appropriate value of those found at the centre frequency is referred to as the bandwidth of the antenna at S11 -10dB [9], [10] and defined as:

$$BW = \frac{f_h - f_L}{f_c} f_c * 100\% \quad (2.7)$$

Where F_h is the higher frequency within -10dB S11, F_L is the lower frequency and F_c is the centre frequency.

2.3 ANTENNA SELECTION

Extensive research is being conducted on the design of on-chip antennas for high band frequencies. These on-chip antenna designs include unbalanced types of antennas such slot and microstrip patch type antennas [11]. Exploratory study and publications on a variety of antennas used for radar and satellite application demonstrate very negative or low gain and low Reflection Coefficient when the antennas aren't combined with a gain enhancement strategy such as the use of reflectors.

The small size of the created device as well as the influence that is caused by the substrate are fundamental problems that generate interest in the ways of feeding, measuring, designing, and fabricating these sorts of antennas. However, in the project that we are working on, we will be using printed technology with a very low dielectric constant. The substrate will be etched, and because this impact will be considered when designing the antenna, we will be able to achieve considerably larger Reflection Coefficient and gains. Gain requirements for short and mid-range radar can be satisfied by an antenna with a gain that is just moderate.

Planar types of antennas are appealing for several reasons, including their low profile, cheap, and easy fabrication. Taking these two considerations into account, the proposed antenna that will be employed for the Ku band short or mid-range system might include a dipole and a microstrip patch antenna, or possibly a planar slot type antenna. In the case of dipole antennas, placing a metal ground at one side of dipole and bending the dipole antennas so that they have a gain of approximately 4-5 dB might further boost the antenna gains. It is possible to achieve a gain of 8 dB using a single patch antenna. Utilizing antennae in an array design allows for a further boost in gain to be achieved. The design of

a printed antenna is investigated in this body of work. In the following section, we will cover the fundamental concept behind microstrip patch antennas.

2.4 PATCH ANTENNA'S WORKING MECHANISM

Microstrip patches are quite popular in the field of wireless technology because they have a low profile, are lightweight, and have a low cost. Recent uses have boosted into the high frequency area, making it suitable for use in applications such as satellite and car radars [11], [12]. A microstrip antenna is made up of a metallic patch that is positioned on top of an electrically thin but physically massive and grounded dielectric (substrate). Microstrip antennas provide a wide variety of appealing benefits like Capable of functioning across a broad frequency spectrum of (0.5 - 60 GHz). Simple to build arrays that are either linear or planar and Easy controlling impedance [10].

Patch antennas can take in a different shape, such as circular, rectangular, ring, disc sector, and annular. Figure 2.6 depicts a rectangular microstrip antenna connected via microstrip transmission line to the main feed line. On a substrate with a thickness of h and having a permittivity of εr, the antenna is printed. On the opposite side the substrate is a ground plane has dimensions that are bigger than those of the patch. It is recommended that the height of the substrate, denoted by h, be a modest percentage of the wavelength of operation (λ), but it should not be significantly less than 0.05. When building a patch antenna for a dielectric with high dielectric constant, such as silicon, however, care should be given to keep the h value as low as possible in order to couple less energy to an undesired mode inside the substrate. This undesirable motion within the substrate, known as a surface wave, has the potential to diminish the antenna's gain as well as its radiation characteristics and cross polarization.

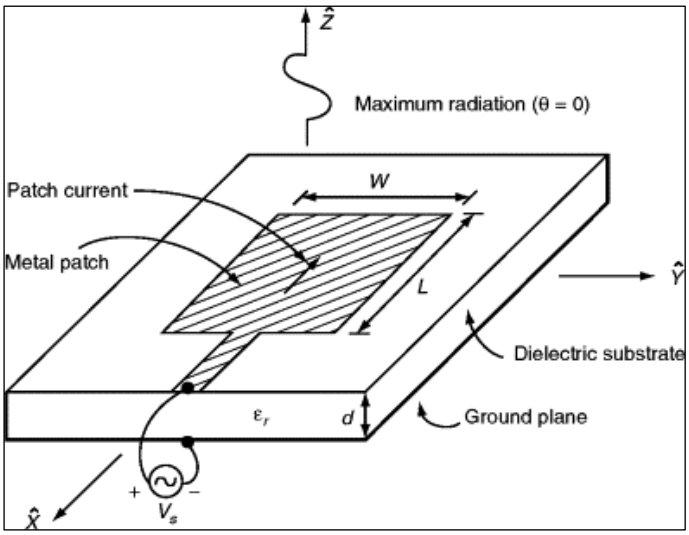

Figure 2.6: Microstrip Patch Antenna Geometric [10].

There are various forms for the radiation element. For circular patches, the centre frequency of operation can be found by the patch's radius; the equation and design explained in detail in the following chapter. However, for rectangular patch antennas, the length L defines the operating frequency [14], and the approximate frequency band can be stated as follows:

$$L_{eeff} \approx \frac{C}{2F_c\sqrt{\varepsilon_{eff}}} = \frac{C}{2F_c\sqrt{\epsilon_0\epsilon_r\mu_0}} \tag{2.8}$$

According to Equation (2.1), the length of microstrip patch antenna must be equivalent one half of the guided wavelength. The wavelength that exists inside the substrate and is shorter than the wavelength that exists in air is referred to as the guided wavelength. The input impedance of the antenna as well as the bandwidth of the antenna are both determined by the width (W) of the patch. The input impedance for a square patch is typically in the range of 300 Ohms. By expanding the width of the antenna, it is possible to lower the impedance while simultaneously expanding the bandwidth. Increasing the patch width, on the other hand, will cause the antenna to become cumbersome and take up a considerable amount of space. Moreover, the antenna's radiation pattern is affected by the antenna's width [14], [15]. The approximately correct expression for the normalized radiation pattern is as follows:

$$E_\theta = \frac{\sin(\frac{KW\ \sin\theta\sin\emptyset}{2})}{\frac{KW\ \sin\theta\sin\emptyset}{2}} \cos(\frac{KL}{2}\sin\theta\cos\emptyset)\cos\emptyset \tag{2.9}$$

$$E_{\varphi} = -\frac{\sin(\frac{KW \sin\theta \sin\emptyset}{2})}{\frac{KW \sin\theta \sin\emptyset}{2}} \cos(\frac{KL}{2}\sin\theta\cos\emptyset)\sin\emptyset \quad (2.10)$$

Where K in the number of free space waves = $\frac{2\pi}{\lambda}$.

The field magnitude can be obtain in formula :

$$f(\theta,\emptyset) = \sqrt{{E_\theta}^2 + {E_\emptyset}^2} \quad (2.11)$$

the following Figure 2.7, illustrate the radiation pattern in both $\emptyset=0^0$ and 90^0 for E-plan and H-plan.

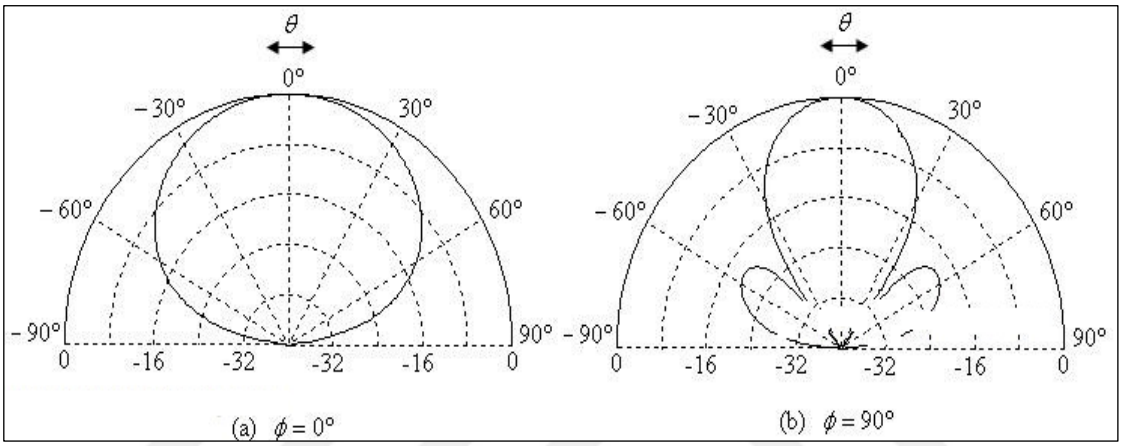

Figure 2.7: Microstrip Patch Antenna Radiation Field [9].

The radiation that is produced by the microstrip antenna is the result of the fringing E-fields that are located on the border of the antenna as explain in figure 2.8 [9], [10]. These E-fields are in phase with one another and add up in phase to produce the radiation. It is essential to have an understanding of the bordering fields in order to comprehend the patch's radiation mechanism. Because the current-distribution on the patch is the opposite of the current distribution on the ground, which cancels each other out, it is impossible for the distribution current on the patch to represent the radiation mechanism. In addition, this could clarify why the microstrip-transmission lines do not radiate. The microstrip antenna emits radiation because of its edges of the patch, which are caused by the favourable voltage distribution; hence, the radiation is caused by the voltage instead of by the current; the microstrip antenna does not radiate electromagnetic energy directly. It is possible to refer to the patch antenna as a "voltage radiator," which distinguishes it from wire antennas, which radiate because of the advantageous current distribution they provide, where the current here add in phase and great the EM field.

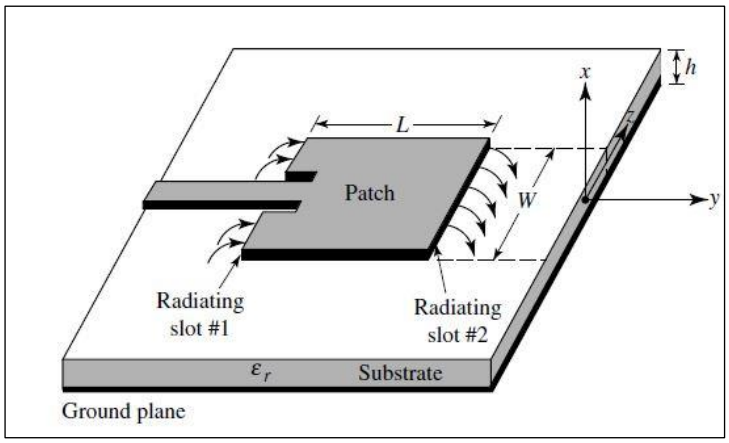

Figure 2.8: The Radiation Edges Mechanize [9][10].

2.5 MPA FEEDING METHODS

When it comes to feeding microstrip antennas, there is a wide variety of possible designs. The microstrip line, the aperture coupling , the coaxial probe, and the proximity coupling are the four that are used most frequently [8], [16].

a. Microstrip line : As was previously explained, a patch antenna has a low current at the end, which results in a high input impedance. It is possible to perform adjustments to the feed and align the antenna impedance to that of a line with 50 ohms [17], [18]. The patch antenna and the strip feed can be made on the same plane. Multiple configurations are possible, including inset feed and quart-wavelength transmission line feed [20].

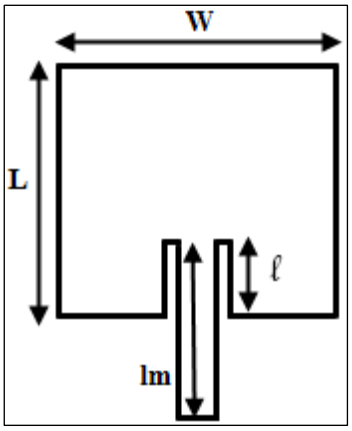

Figure 2.9: Inset-Feed Patch [18].

Figure 2.9's inset distance could be utilized to change the antenna patch's feeding impedance matching [18]. The below equation for rectangular MPA inset can be used as

a guide for a certain operating frequency [19]. the Current with sinusoidal distribution, and a distance A away from the end should increases the current by a factor of $\cos\frac{\pi A}{L}$. when the A length is equal to $\frac{L}{4}$. So, the $\cos^2\frac{\pi A}{L} = \frac{1}{2}$ then 1/8 inset feed will decrease the impedance by half.

$$Z_{in}(A) = \cos^2(\frac{\pi A}{L})Z_{in}(o) \quad (2.12)$$

Figure 2.10 indicates that a quarter-wavelength approach with characteristic impedance Z_c can be used to match the microstrip antenna to a transmission feed line with characteristic impedance Z_o.

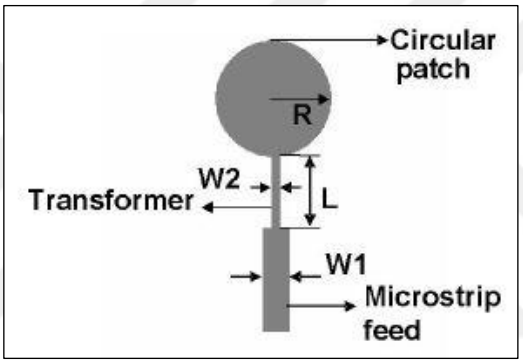

Figure 2.10: Quarter-Wavelength Technique [21].

The single-section quarter-wave converter has a length equivalent to a quarter wave in microstrip, and its characteristic impedance, Z_C, may be calculated using the formula (2.13).

$$Z_c = \sqrt{Z_o Z_{in}} \quad (2.13)$$

Where Z_0 is 50 Ohm characteristic impedance feed and Z_{in} is the input patch antenna impedance.

b. Coaxial Cable / Probe Feed : Figure 2.11 shows how to use a coaxial cable to feed a probe, with the inner conductor connected to the radiation patch antenna and the outer conductor grounded [22]. Although coaxial feeding is advantageous because to its low bandwidth and ease of implementation, minimal spurious radiation, and ease of matching,. Similar to an inset feed, the position of the Coaxial connector can be altered to obtain 50 Ohm input impedance [10]. Regarding the inductance introduced by the

coaxial feed, care must be given. To disregard the influence of inductance, the substrate's height h should be believed to be low. Additionally, the probe will emit radiation, which may be directed in unwanted directions.

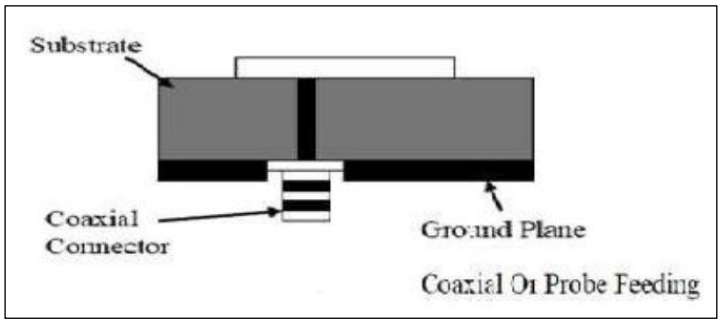

Figure 2.11: Geometric of The Coaxial Feed [22].

c. Aperture coupled Feeds**:** Aperture coupling is a relatively new method of non-contact feeding. It is made up of 2-substrates that are isolated by a ground-plane. On the lower substrate's underside is a microstrip line feed whose energy is connected to the radiated element through a ground plane slot (Figure 2.12) [23]. The drawback of this approach is its increased fabrication difficulty.

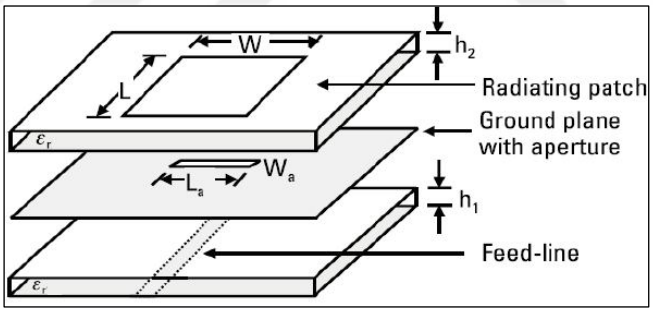

Figure 2.12: Geometric Of Aperture Coupled Feed [32].

d. Proximity coupled feed: Proximity coupling has the greatest bandwidth and the least amount of spurious radiation. The principle of its connection mechanism is capacitive [24]. The length of the feeding stub and the (width to length) ratio of the patch are utilized to regulate matching. Due to the usage of different dielectric layers that require perfect alignment, it is harder to produce this method, and the antenna becomes thicker as a result as illustrate in Figure 2.13.

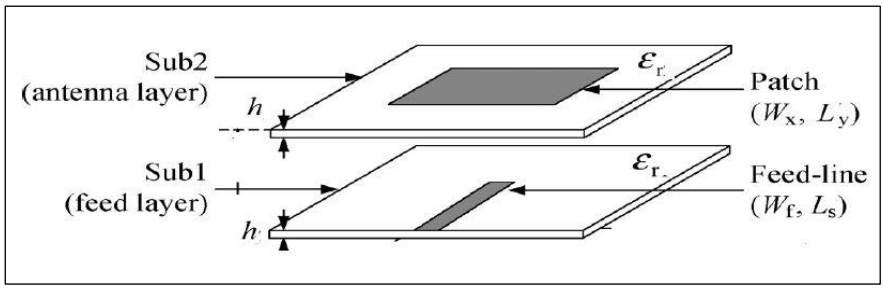

Figure 2.13: Geometric of The Proximity Coupling Feed [24].

2.6 MICROSTRIP ANTENNA ARRAY FEEDING NETWORK

A wide variety of spatial layouts for multiple antennas can produce high characteristic and Mutable form patterns. "Arrays" is the term used to describe these sets of antennas. The electromagnetic fields produced by an array antenna's individual elements contribute in certain directions and subtract in others. There are a variety of feeding network according to the application and the requirements. nevertheless, here we will give a short introduction to the most kind of feeding networks used in radar and satellite applications. microstrip patch antenna arrays are typically configured with series and corporate feed networks as their two primary types of feeding networks. The corporate feed networks illustrated in Figure 2.14 are the microstrip patch antenna array layout that is considered to be the most advantageous. Each element of the array includes its own feeder line, and these lines are joined to the other lines in the array through two-way combiners [25].

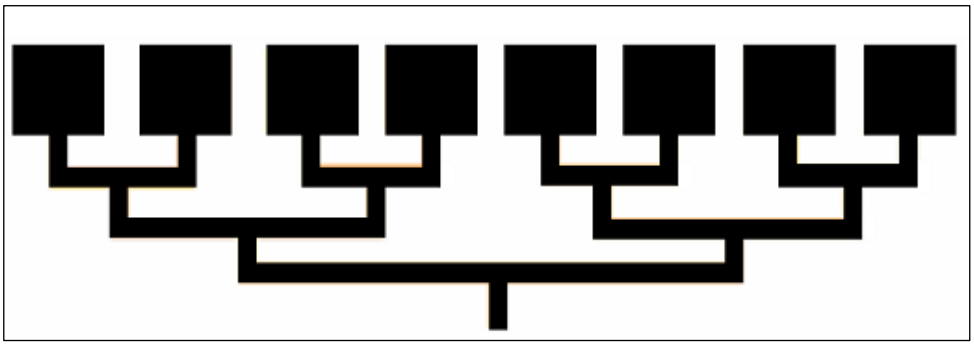

Figure 2.14: Corporate Feed Network Geometric [50].

However, they take up a significant amount of space, the vast lengths of lines that are employed result in significant losses, and the discontinuity that occurs between line corners results in significant mutual coupling impacts that alter the radiation patterns.

Another form of structure utilized in microstrip arrays is the series feed network. In these types of setups, a single transmission line serially feeds antenna patches. This feeding architecture minimizes feed line lengths, which is a crucial criterion for antenna performance [26]. There are two typical applications for series feed arrangements. Figure 2.15 depicts a shunt-connected series feed, also known as an out-of-line feed. A number of feeding lines extend outward from the primary feed line, and an antenna element is attached to the terminal of each individual feeding line. While Figure 2.16 depicts an in-line feed. This category of networks is characterized by having a core feed line, and the members are directly loaded on this line in sequential order [26], [27].

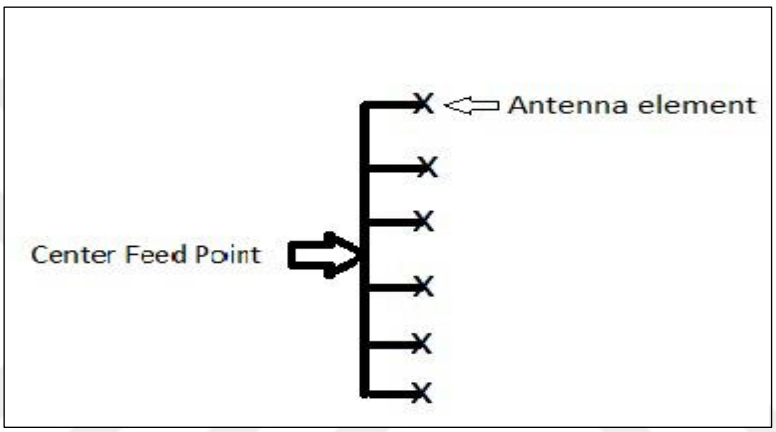

Figure 2.15: Series Feed-Shunt Connect [50].

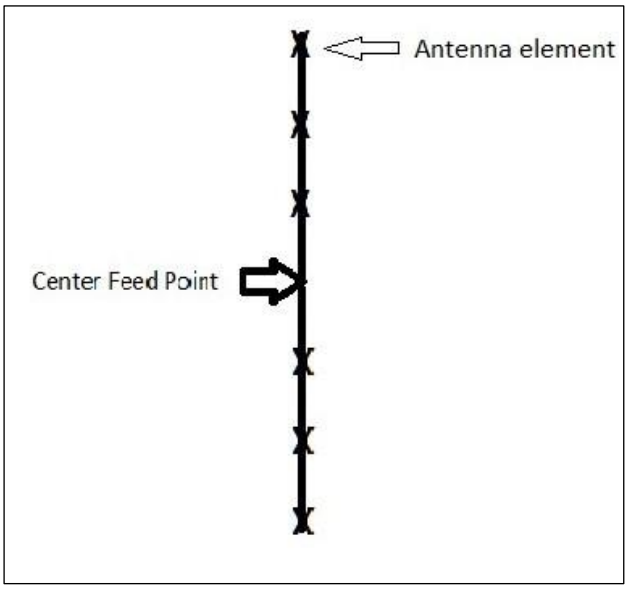

Figure 2.16: In Line Feeding Network [50].

Series and corporate feed are the most common feeding network for microstrip antenna arrays. The series feed has a smaller dimension and less feed radiation, however the bandwidth of the antenna is fixed and the excitation of a single element will influence the excitation of the entire antenna array [10]. In contrast, corporate feed has greater control ability over the amplitude and phase of the radiating element, achieves a better gain and a narrow beamwidth, but has a larger feedline radiation.

2.7 LITERATURE REVIEW

Highly directional patterns can be produced by arranging several antennas in space in a variety of geometrical configurations. increasing the gain characteristics, bandwidth and sidelobe level of the antenna is vital automotive radar and even for satellite, as the radar's radiating power is proportional to the antenna's gain [28]. Planar antenna arrays with a low profile and small weight are favoured for such applications [29]. Furthermore, in Radar a greater radiating power can obtain a longer detection range and better image quality. high gain antennas can extend the detection range and improve the resolution by offsetting the effects of the high propagation loss throughout the microwave and millimetre-wave spectrum and the power consumption of the transmitter and receiver [30]. In addition, for radar application, the bandwidth represents the detecting target's resolution. Every frequency in this miner corresponds to a pixel in the reflected image.

There are various research on gain, bandwidth enhancement and sidelobe elimination. In [31], a grid antenna array for short-range Automotive radar V2V and V2S (vehicle-to-vehicle and vehicle-to-satellite) has been designed on a substrate with a thickness of 1.6mm and relative high dielectric constant of 3.0. This design has achieved a gain of 14.2 dBi and an SLL of -16.3 at a centre frequency of 24 GHz for V2V detection. In contrast, the design record for V2S is 10.4 dBi of maximum gain and 80% efficiency in the operating region of 17.3-17.8 GHz. In [32], -20 dB low SLL and 13.5 dB gain achieved by using multi-layer substrate antenna design. 10x8 planar SFPA array for Automotive radar using with SIW integrated waveguide in [33] obtain SLL -16 dB in E-plane and -14 dB in H-plane. A new 2x16 array Ku band patch antenna design with two symmetrical slits in [34] achieved -22 dB SLL in H-plane and -11.5 in E-plane. 2x4 FMCW antenna for radar application obtain -15 dB SLL and 12.5 dBi gain with relative BW more than 1.5 Ghz reported in [35]. However, The double layer improves the BW but increases the thickness

of the PCB. The work in [36] presented rectangular MPA array using 96 radiating element with large space achieved -20.9 dB SLL and 22.26 dBi gain used in 24 GHz radar for avoiding collisions.

In [37] present a series feed design for Automotive radar, The highest SLL in E-plane are -12 dB, -15 dB at 76 GHz and 77 GHz. however, These values decrease incrementally with increasing frequency. The peak gain measured 20 dBi, 19.2 dBi at 77 GHz and 76 GHz respectively. A dual-layer (PCB) designed for automotive radar has been reported in [38], The major feeds of SIW slot and co-planar transmitting array archives gain 18.5 dBi at 76.5 GHz. Nevertheless, The combination of SIW and Co-planer requires a volume, even if the area involved is very modest. the gap between the antenna and the 4-ports SIW makes the overall design bulk thickness. SIW has received a significant amount of attention as a result of the several benefits it offers in the form of low manufacturing costs, reduced radiation losses, and relative high density integration in its design.

SIW single-layer has 32x4 slot elements in its configuration in [39] obtain gain 2.8 dBi, -21 dB SLL and 67% efficiency with maximum S11 -11.5 dB over the operation band. W-band antenna consisting of a 3D printed slotted waveguide array with a total of 12 radiating components and a differential feed configuration has presented in [40], Considering the idea of using 3D metal design for the first time in Automotive radar the antenna obtain 12 dBi and SLL -19 dB. However, for driver assistance the possibility of its integration with the vehicle remains an important matter.

The simulated results in [41] of a 24GHz millimetre wave microstrip antenna array with 6x8 elements constructed on Rogers4350 provide a narrow bandwidth of around 250 MHz, 20.56 dBi gain at 24 Ghz, and -18 SLL. a corporate feed in [30] 64 E-shape patch design for FMCW automotive radar proved a good gain enhancement 25.2 dBi at 24 GHz centre frequency and -14 sidelob level with bandwidth close to 1 Ghz. Furthermore, In order to get the highest possible gain and prevent the formation of gating lobes, the spacing elements has been set to 0.80λ on both the E-plane and the H-plane. Furthermore, in the next chapter of antenna design, the comparison with related works and the contribution of the thesis are considered.

3. ANTENNA DESIGN PROCEDURE

3.1 INTRODUCTION

This chapter will examine the design of patch antennas operating Ku band spectrum. Because of its ease of usage and compatibility with current printed circuit board technology, microstrip antennas are among the most common types of antennas used in the microwave frequency spectrum. The challenges of constructing wide bandwidth antennas on very thin substrates with a lowest existence dielectric constant. As described in the preceding chapter, the design of patch antennas and analytical methods exist for this purpose. However, this method can be utilized for patch antennas on homogenous substrates, not etched substrates; etching technique will be used to obtain a low-profile substrate and enhance antenna gain and directivity. Microstrip antennas have a number of drawbacks, the most significant of which are their narrow bandwidth and relatively low gain. The low profile of the antenna contribute further to the deterioration of these two properties. The reason for this is that the antenna's size, bandwidth, and efficiency all have a basic connection with one another. Neither the operating bandwidth nor the antenna efficiency can remain constant as antennas get smaller. Smaller antennas often have less gain than their larger counterparts because of this size-gain relationship. Increasing gain and bandwidth is possible by using etching, DGS or any other techniques. However, for significate increasing in Antenna characteristic, The array configuration have been utilized recently in many application.

3.2 METHODOLOGY

The first step in creating an antenna is to select an antenna kind and dielectric substrate that are compatible. For initial, the proposed antenna type is a microstrip antenna. Microstrip antennas may have the advantage of being integrated into microwave integrated circuits. The array design steps are determined in accordance with the project specifications. Figure 3.1 depicts the design process.

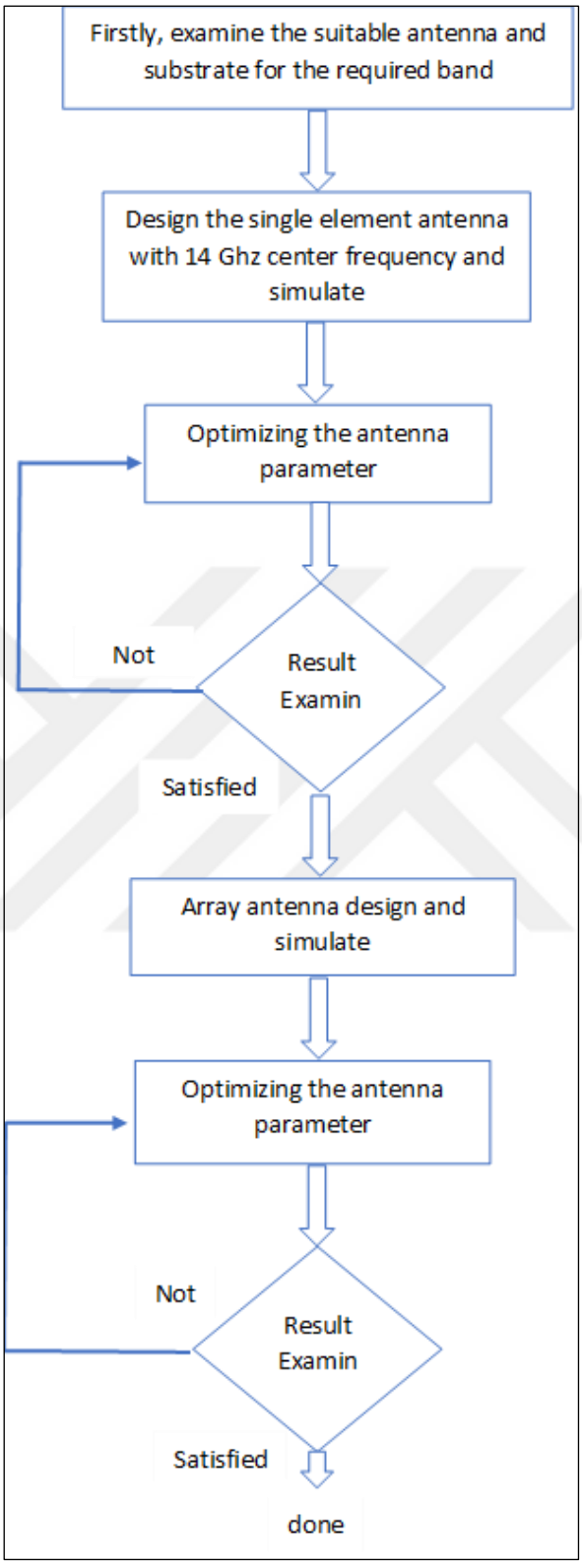

Figure 3.1: Design Process.

3.3 SUBSTRATE FEATURES IMPACT

The dielectric constants (ε_r) of the numerous substrates available for use in microstrip antenna design typically fall within the range of 2.2 to 12. The substrate thickness parameters used in microstrip antenna design are shown in Table 3.1. For optimal antenna performance, thick substrates with low dielectric constants are preferred because they allow for higher radiation efficiency, wider bandwidth, and less constrained fields during transmission over space [42][43]. however, These benefits are paid for with an increase in dielectric loss, element size, weight, wave propagation loss, and unwanted radiations. In the other hand, thin substrates with greater dielectric constants are typically favored since they required tightly bound radiation to avoid unwanted radiation and coupling, resulting in reduced radiating element size [42][43].

Nevertheless, they have a lower bandwidth and a lower overall efficiency. Because of this, the accepted methodology for the design of antennas calls for a compromise between bandwidth and efficiency.

In this work, a substrate with a very low dielectric constant has been used. In contrast to conventional paper works, not only is the dielectric here extremely low, but the thickness is also very low. Therefore, it is challenge to achieve high efficiency, broad bandwidth, and high gain. The goal behind the selection of these substrate futures is to obtain the greatest outcomes from low dielectric and thin thickness with considering to decrease the undesirable effect of thin substrate and low dielectric losses. Rogers RT5880LZ Lossy with 2.0 dielectric constant and 0.0021 tangent loss with substrate thickness 0.5mm have been used in this work.

Table 3.1: Substrate Properties [42].

Thick Dielectric Substrate	Thin Dielectric Substrate
Low dielectric.Constat, better efficiency, wider BW, big Size, massive weight, and high dielectric losses.	High dielectric. Constant, efficiency less than in Thick, Size reduction, Lightweight and minimum loss of dielectric

3.4 SINGLE ELEMENT DESIGN

Microstrip Patch Antennas come in a variety of forms. This antenna uses the circular shape. Microstrip antennas have found widespread application in microwave frequency spectrum and have been integrated into a variety of electronic products in recent years [44]. These devices are widely used because of their small form factor, versatility, low cost, and simple printed circuit board technology [45].

The formulae [10], [46] describe the resonant frequency of a circular patch as illustrate in equation (3.1) :

$$A = \frac{F}{\{1+\frac{2h}{\pi\varepsilon rF}[ln(\frac{\pi F}{2h})+1.7726]\}^{1/2}} \tag{3.1}$$

$$F = \frac{8.791*10^{9}}{Fr\sqrt{\varepsilon r}} \tag{3.2}$$

While (F_r) is the patch's resonance frequency and (ε_r) the substrate's relative permittivity. And as well as Ae, the diameter of the circular patch's effective area, formula in (3.3) [46].

$$Ae = A\{1 + \frac{2h}{\pi\varepsilon rA}[ln(\frac{\pi A}{2h}) + 1.7726]\}^{1/2} \tag{3.3}$$

Table 3.2 displays the dimensions of the antenna and its direct microstrip feed line. The antenna was designed using Rogers RT5880, which has a thickness 0.5mm, a Dielectric Constant (εr) 2.0, and an electric loss tangent 0.0021.

Table 3.2: Single Element Antenna Design Specification.

Parameter	Value
Operating frequency	14.4 GHz
Substrate material	Rogers RT5880LZ Lossy
Substrate area	15mm*18mm
Substrate thickness	0.5 mm
Dielectric Constant (εr)	2.0
Antenna radius (a)	4.1 mm
electric loss tangent	0.0021

There are numerous patch feeding techniques. In this project, inset feeding was chosen over coaxial feeding for the circular patch since coaxial feeding is incompatible with array

design. Moreover, inset fed approaches provide a higher purity polarization with few dB [30].

This section describes the design process for the proposed High gain and directional microstrip antenna. It started with the design of a conventional circular patch at frequency more than 14.4 GHz center frequency with 50 Ohm impedance using microstrip line as shown in Figure 3.2a. The suggested antennas design has been optimized through simulation using CST microwave studio. The results of the simulation of the S11 across the antenna operating band are depicted in Figure 3.6. The conventional design has recorded Reflection Coefficient (S11) –31 dB, side lob level –12dB, gain 7 dBi.

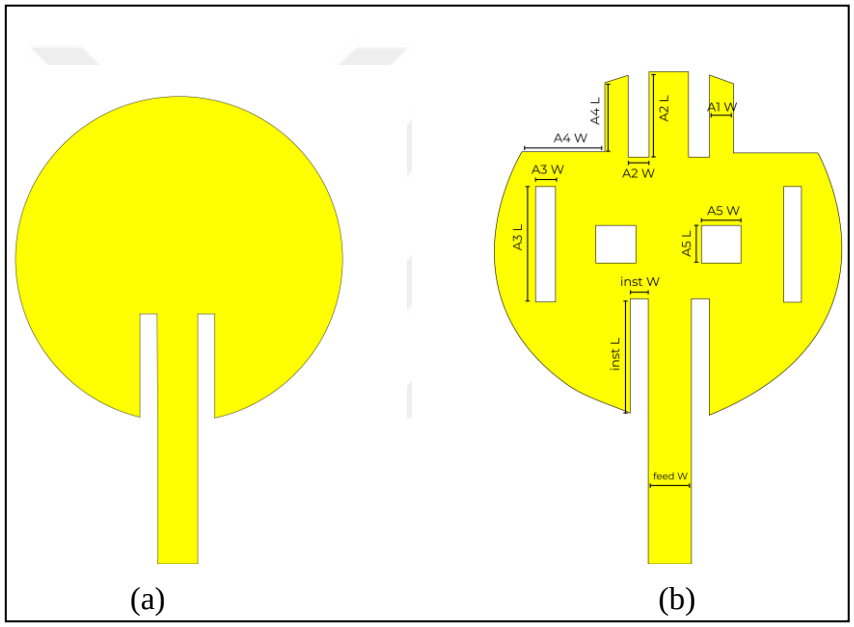

Figure 3.2: Antenna Geometric (A) Conventional Design, (B) Novel Design.

In contrast to the rectangular shape of the patch, changing the impedance of the circular shape is a little more complicated. As mentioned previously, the resonance frequency is primarily dependent on the length of the patch, whereas the width can be altered, thereby allowing the impedance to be changed to fit the design.

The only variable in circular patch to determining the resonance frequency of a circular structure is the radius. As shown in Figure 3.3, the Normalized impedance at 14.4 GHz requires additional improvement in order to reach the fit value of 50 ohm. The minimum S11 value for the conventional patch falls at 14.7 GHz as illustrate in Figure 3.3. Changing the patch's radius may modify the impedance curve, but it also shifts the center frequency.

The inset fed of the patch can penetrate further inside the patch to achieve the needed impedance at the center frequency, however it will have an effect on the radiation characteristics such as SLL and angular width as the inset fed that reaches the center of the patch.

Here, we aimed to develop an alternative method for controlling the impedance of a circular patch without altering its radius. A shown in Figure 3.2b, Four geometric slots on the have etched from the patch. The variation of the impedance (impedance control) as well as the position of the initial frequency resonance of the novel geometric patch antenna in relation to the parameter A1W. the 50 Ohm normalized impedance at the center frequency achieved with A1W = 0.5mm at 14.4 GHz and without modifying the value of the patch radius. Figure 3.4 depicts the effect of increasing the A1W sweep from 0.4 mm to 1.1 mm.

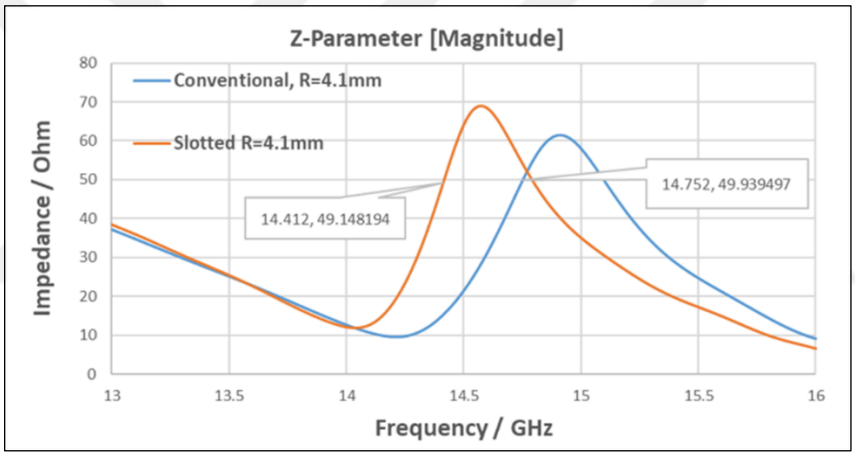

Figure 3.3: Impedance Curve For The Conventional Design.

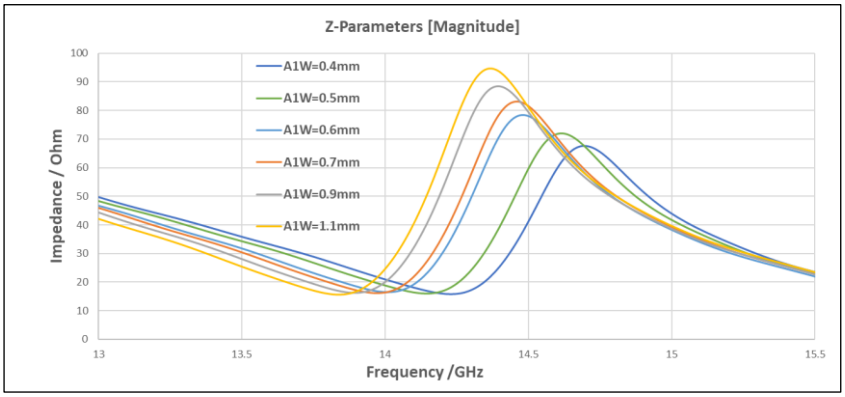

Figure 3.4: The Variation Of The Impedance Effected By A1width.

According to the preceding research, the proposed antenna's initial resonance mode has a link with slots. Consequently, further analysis is required between resonance frequency and slot form (A2,A3,A4,A5). In this parametric study, just one variable was varied at a time, while the others remained unchanged. Figure 3.5 depicts the correction of the S11 while sweeping the parameters of the slots.

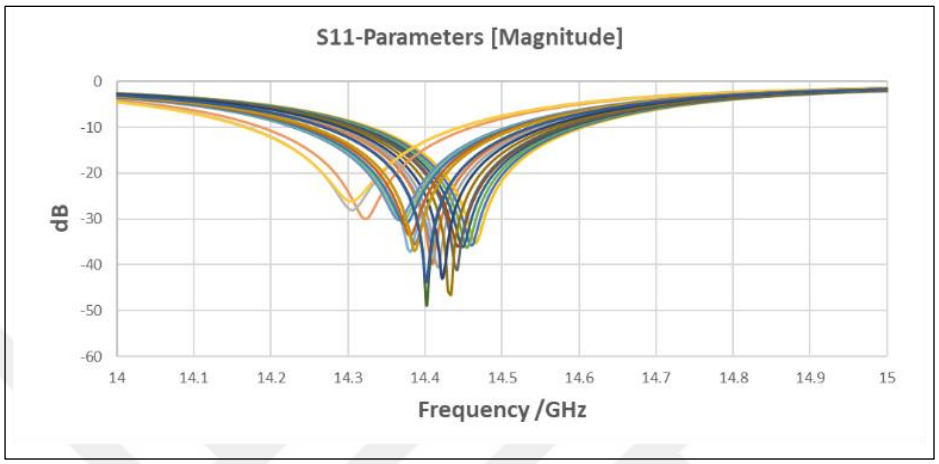

Figure 3.5: Reflection Coefficient (S11) Correction.

Based on the findings of the current study, a compact microstrip antenna has been built using a microstrip feed line and a single-layer patch element. The final simulated Reflection Coefficient (S11) reach to –49 dB done by adjusting the slot's length, width, and placement shown in Figure 3.6. In addition, distributed current demonstrates that the suggested antenna's impedance matching at the operating frequency is stable. Figure 3.7 illustrates the distribution of antenna current at the resonance frequency of 14.4 GHz. At the patch antenna's resonance frequency, the highest current is observed to be spread between the slots.

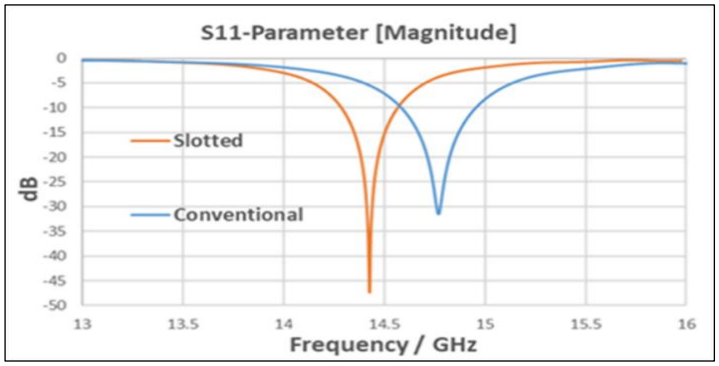

Figure 3.6: Reflection Coefficient (S11) Of Conventional and New Design

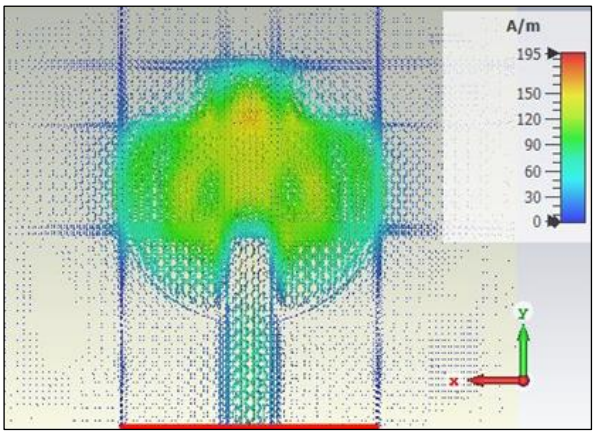

Figure 3.7: Current Distribution At 14.4 Ghz.

almost, the changing in the conventional patch geometric design with slots (in radiated patch) or (in the ground plan such as DGS technique) may produce another resonant frequency. this could be an advantages in many multi-band application.

Nevertheless, in Automotive V2V and V2S satellite application, The single resonant and wide BW are preferred. from the previous results the antenna performance proved with single band operation. Moreover, the rectangular slots impact focus on the characteristics improvement in impedance, efficiency and Reflection Coefficient. In addition, the novel design have keep the same characteristic of directive pattern of the (H-field) and (E-field). Figure 3.8 (2D-E-field pattern) for the slotted design.

The side lobe level at Phi = 90^0 improved from –12 dB in the conventional to -14 dB in the slotted design. Figure 3.9 show the (conventional & slotted) 3D field pattern and the small different by –2 dB in SLL.

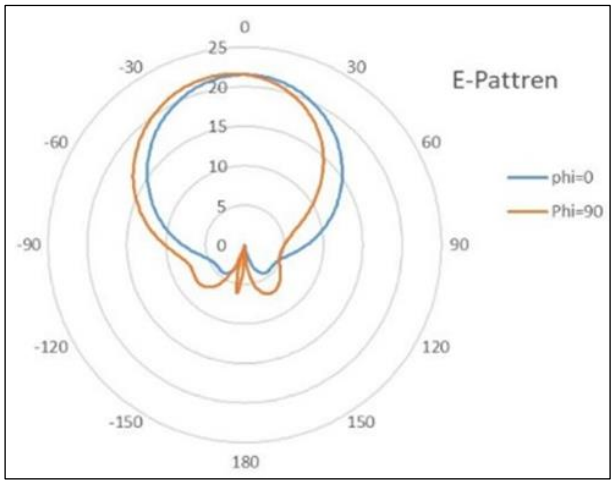

Figure 3.8: 2D E-Field For The Slotted Patch.

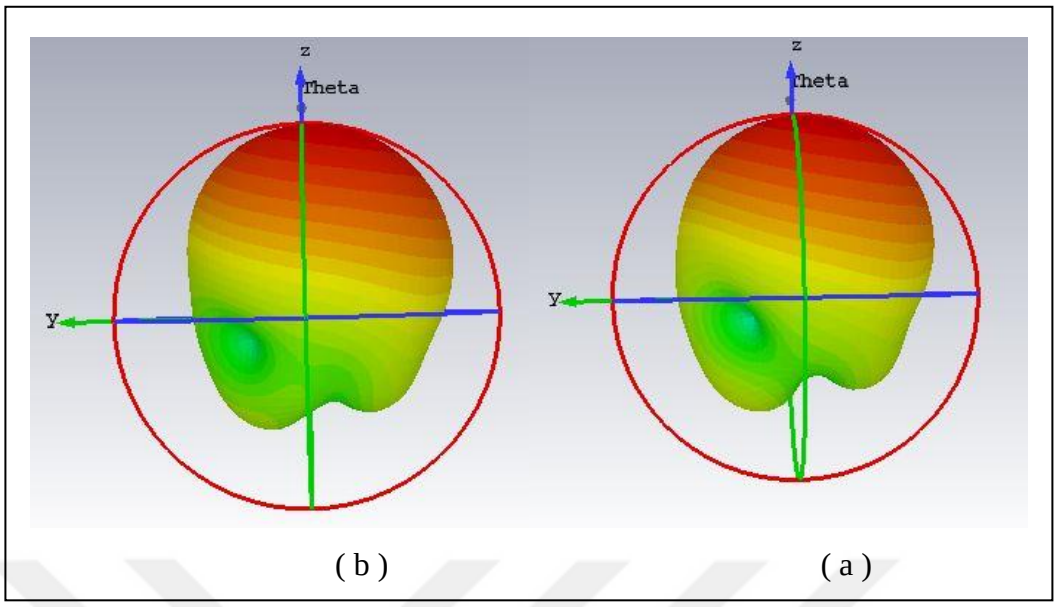

Figure 3.9: 3D Field Pattern (A) Conventional Design (B) Novel Design.

The exact optimization the dimensions of the slots, as detailed in Table 3.3. Table 3.4 demonstrates the enhancements made to antenna impedance, S-parameters, gain, directivity, and side lob level (SLL).

The properties of the dielectric constant were explained at the beginning of the design process, and two routes were presented: one in which the dielectric constant was low and the thickness was high to obtain a wide bandwidth, and another in which the dielectric constant was high and the thickness was thin to achieve the minimum dielectric loss. In this work, we employ a different approach, selecting a very low dielectric constant of exactly 2.0 to ensure optimal efficiency performance. The thin substrate was selected due to its low (dielectric and tangent) losses properties. The power losses are explained in Figure 3.10, and the total power that was simulated is 0.5 W; with this information, we can determine the total amount of power that was lost. The curve of the dielectric loss shows that the antenna recorded the minimum loss value, with the highest loss record at the resonant frequency equal 0.033 W, which is the minimum value that may be used in antenna design. As shown, the highest radiated power is 0.38 watts, which is equivalent to 76% of the power accepted. The remaining 0.12 watts of loss power is distributed among several sources (dielectric loss, metal loss, port absorbed and power outgoing the port). On the other hand, for a single patch and directed pattern, this is considered of as a very good efficiency performance for thin substrate with low dielectric constant . In addition to this,

the next array design features a significant improvement to the efficiency with which it radiates energy.

Table 3.3: Exact Slots Dimensions.

Parameters	Unit (mm)	Parameters	Unit (mm)
Radius (a)	4.1	A2 width	0.5
Inst length	2.85	A3 length	3
Inst width	0.5	A3 width	0.5
A1 width	0.5	A4 length	1.9
A2 length	2.15	A4 width	2.6
A5 length	1	A5 width	1

Table 3.4: Novel And Conventional Simulated Metrics. Comparison.

Parameter	Novel design	Conventional design
Center frequency	14.4 Ghz	14.7 Ghz
Reflection Coefficient (S11)	–49 dB	–31 dB
gain	7 dBi	7 dBi
SLL Phi=90^0	–14.1 dB	–12.9 dB
Tot. efficiency	76%	69%
Bandwidth	285 MHz	327 MHz

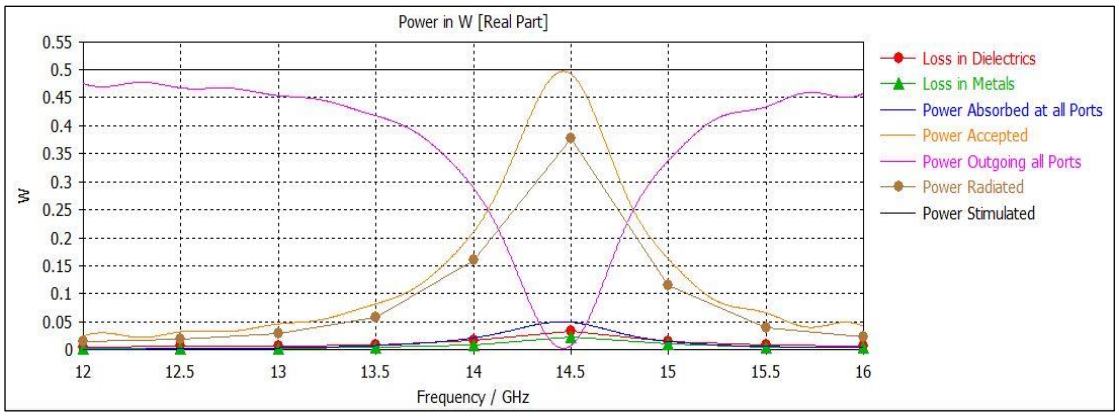

Figure 3.10: Single Element Power Losses Coefficients.

4. ANTENNA ARRAY DESIGN

4.1 ARRAY ANTENNA

Highly directional patterns can be produced by arranging several antennas in space in a variety of geometrical configurations. Boosting the antenna's gain characteristics and SLL is essential for satellite and vehicular radar since the gain directly affects the radar's radiating output [28]. Planar antenna arrays with a low profile and small weight are favored for such applications [29]. Furthermore, in Radar a greater radiating power can obtain longer detection range and better image quality. high gain antennas can extend the detection range and improve the resolution by offsetting the effects of the high propagation loss throughout the millimeter-wave spectrum and the power consumption of the transmitter and receiver [30].

Feeding networks that use a series feed and a corporate feed are the most typical for microstrip antenna arrays. The feed radiation from the series configuration is lower and the dimensions are smaller. The antenna's bandwidth is fixed, though, thus exciting one element will affect the excitation of the rest of the array. The corporate feed, on the other hand, allows for more precise regulation of the radiating element's amplitude and phase, improves gain and narrows beamwidth at the expense of a more substantial feedline radiation footprint.

4.2 1x4 SHUNT-SERIES FEED ANTENNA ARRAY

The proposed array design has simulated by using CST microwave studio and fabricated on rogers RT5880LZ lossy with Dielectric Constant (εr) 2.0 and substrate thickness 0.508 mm. Figure 3.1b depicts the shape of the single element utilized to construct the suggested array. The linear array consists of identical patches with fixed spacing distance of (d) from center patches.

Reflection Coefficient (S11), bandwidth, directivity, efficiency, and gain have all been significantly enhanced by the new array design. The schematic for a 1x4 array, which consists of four antennas and a single feed line, is shown in Figure 4.1.

The mainlines characteristic impedance (B2) is set to 100 Ohm in order to reduce feedline radiation. The transmission line's width is then determined using equation (4.1) and optimized using simulation CST [47]:

$$Wf = \left(\frac{377}{Zo\sqrt{\epsilon r}} - 2\right) h \tag{4.1}$$

In order to achieve the match between the main feedline and each patch, the quarter wave transformer Zm (B1W,B1L) was added to the single element feedline. The Zm length, width, and impedance are calculates and optimized to be 2 mm, 2.1 mm, and 46 ohm, respectively with electrical length = 46^0, resulting in S11 improvements of -37 dB, 422 MHz BW from 14.68 GHz to 15.1 GHz, and SLL of –21.3 dB. Figure 4.2 show the effect of B1W width varying from 1.8 mm to 2.1 mm on the Reflection Coefficient (S11).

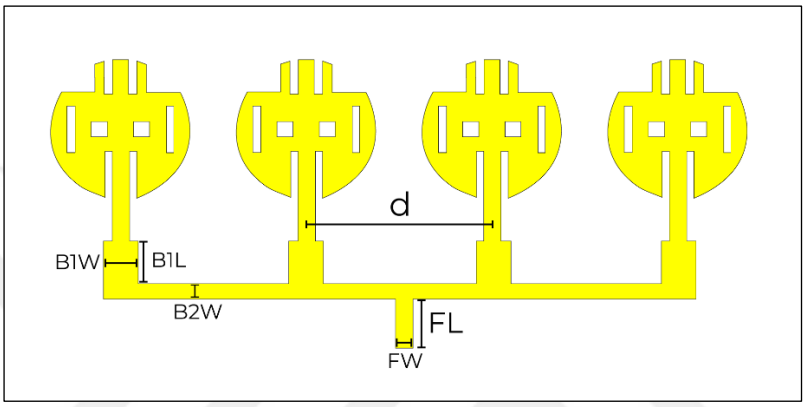

Figure 4.1: 1x4 Shunt-Series Antenna Array Design.

Transmission lines of the feeding network have a significant impact on radiation, center frequency, S11 (Reflection Coefficient), and overall patch gain in array antenna design. As a result of this, thinner and minimization of the feed line network are required.

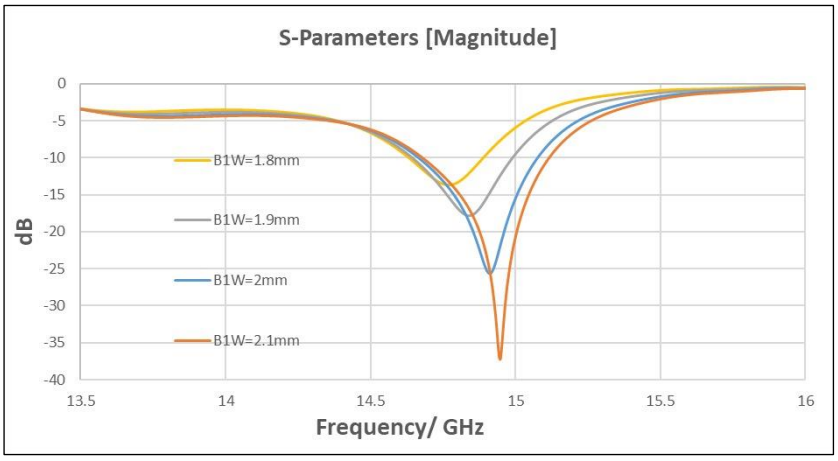

Figure 4.2: 1x4 Antenna Array (S11) effected By B1W Impedance Width Sweeping.

One of several types of controls that can be used to affect the overall pattern of the antenna system is the relative spacing between radiating elements [48]. In order to determine how

the antenna's main lobe's directional pattern compares to that of the other lobes, SLL measurements must be taken. SLL is a crucial indicator for many satellite and radar uses. Main lobe pattern and antenna performance both improve with decreasing side lobe peaks [49].The wavelength of the antenna's radiation close to λ= 20.9 mm. Therefore, the spacing between centers should be λ/2 = 10.4 mm or λ/4 = 5.2 mm. However, the radius of the single-element patch is 4.1 mm, thus center-to-center should be at least d=0.39λ. In the Figure 4.3 below, the influence of spacing (d) on the radiation characteristics and SLL of an array antenna can be observed. the 1x4 antenna design achieved –21.1dB low side lobe level obtain in (H-field and E-field). A simulation was conducted with the distance d varying from d=(0.445, 0.52, 0.56)λ. It has been demonstrated that the spacing between elements must be around to λ/2.

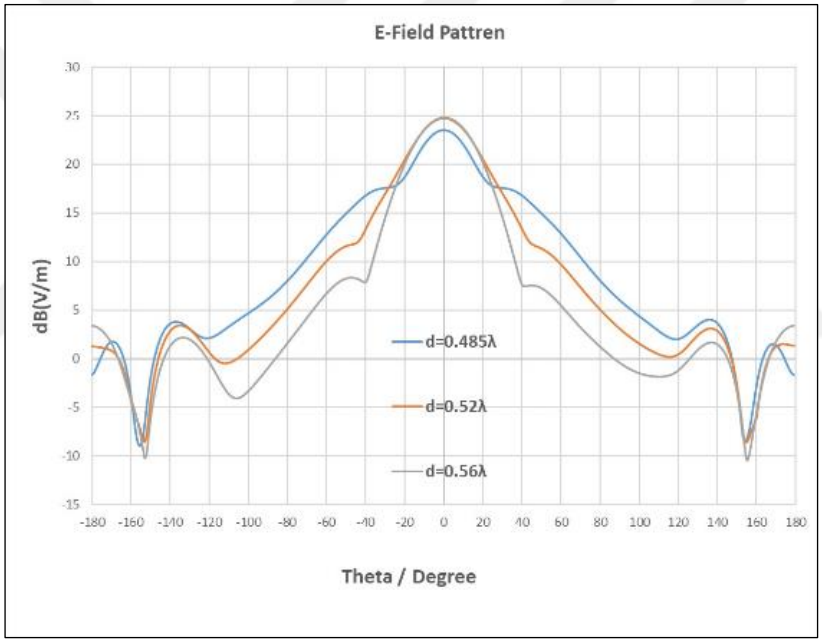

Figure 4.3: Simulated E-Field Pattern Conducted With Distance D.

For optimal performance, the parameters described in Table 4.1, are adjusted and fine-tuned in accordance with the optimal effect while maintaining the maximum S11 at frequency of 14.9 GHz. As the simulated S11 shown in Figure 4.4 provides BW from 14.68 GHz to 15.1 GHz with –37 dB S11. Changing these settings causes an impedance mismatch and an increase in mutual coupling effect. The antenna achieved gain 10.8-11.5 dBi at the operation band with minimum value 10.1 dBi as despite in Figure 4.5 Moreover,

the Figure 4.6 illustrate the 2D E-field and H-field pattern show the directivity of the design antenna in addition to the compressed sidelobe level.

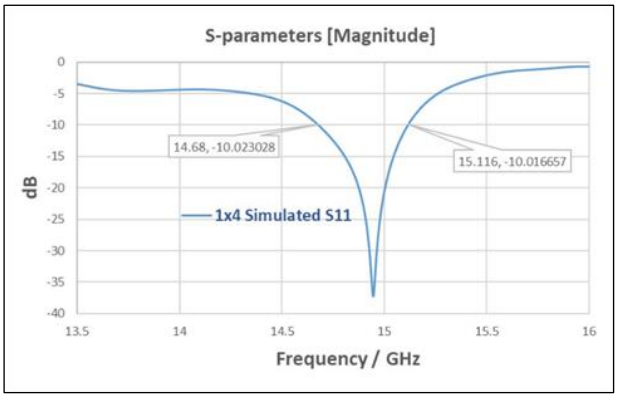

Figure 4.4: 1x4 Reflection Coefficient (S11).

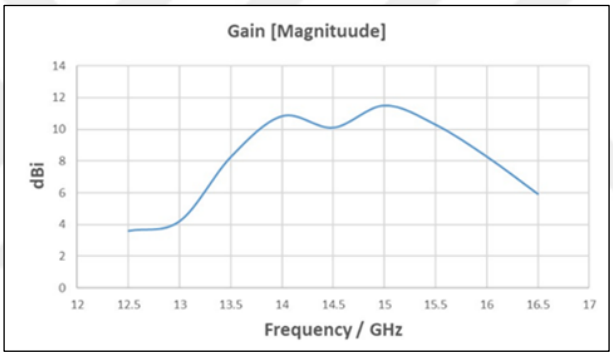

Figure 4.5: 1x4 Antenna Gain

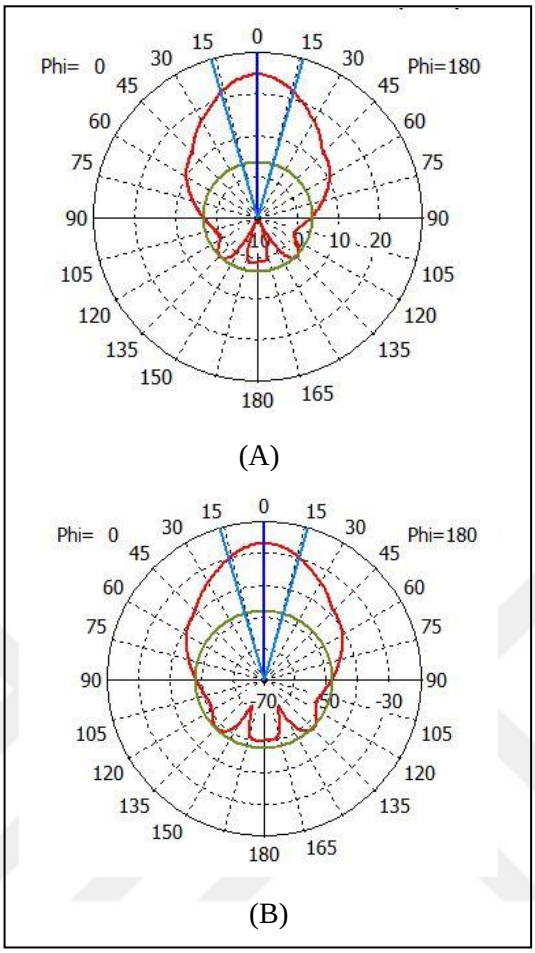

Figure 4.6: 1x4 2D (A) E-Field And (B) H Field.

Table 4.1: 1x4 Fed Network Dimensions.

Parameters	Unit (mm)	Parameters	Unit (mm)
d	11	B2W	0.5
B1W	2.1	B2L	35.1
B1L	2	FW	1
		FL	2.7

Figure 4.7 illustrates the large improvement in antenna array efficiency and the significant drop in power losses. The array design has reached 0.027 W as the minimum value of dielectric losses at the center frequency, which is a significant improvement for array design over the single element design. as shown, the highest radiated power is 0.43 W, which is equivalent to 86% of the power applied. While the variation of the efficiency over the operation band was 75% as a minimum to 86% as a maximin recorded at the center frequency band.

From the power accepted curve, the antenna has a very good impedance matching while the power accepted by the antenna at the operation band very closed to the power applied, and the power compressed out of the band designed. This explain the means of the power reflected and the suitable reactive of the reflection coefficient over the required band. Table 4.2 illustarte the matrix imoriment from single element to 1x4 array.

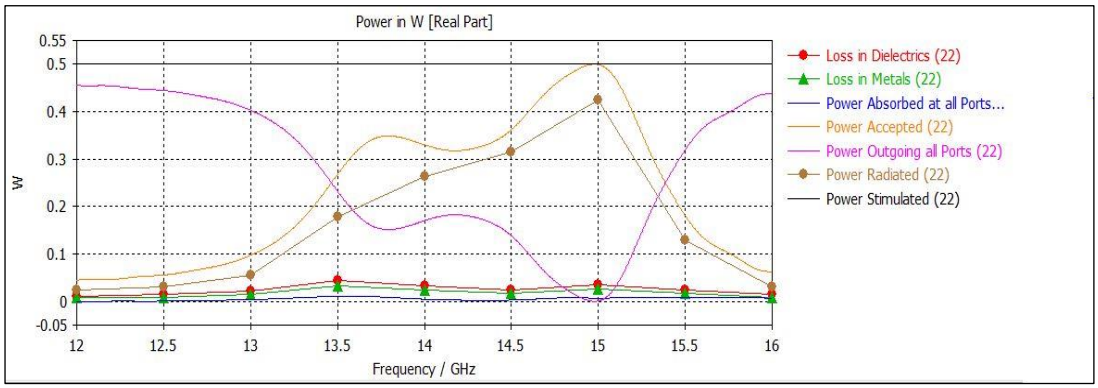

Figure 4.7: 1x4 Array Power Losses Coefficients.

Table 4.2: 1x4 Array Metrics Improvement Compared To The Novel Single Element.

Parameter	Gain	Directivity	S11	Rad.Efficiency	Sidelobe level	Bandwidth
Single/element(Novel)	7 dBi	7.98 dBi	–49 dB	76%	–14.1 dB phi=90^0	285 MHz
1x4 Array deign	11.3 dBi	12 dBi	–37 dB	86%	–21.3 dB	422 MHz

4.3 3x4 SHUNT-SERIES ANTENNA ARRAY

It's critical to consider the radiation intensity for the directed pattern. Since then, the radar and satellite industries have recognized the required significance of high gain. the gain can improved by increasing the number of element in array. The array design could be configure in 2D demission. In this regard, as shown in Figure 4.8 3x4 antenna array have designed and simulate. the feeding network designed With an equal power division between the 3 rows and equal spacing between elements.

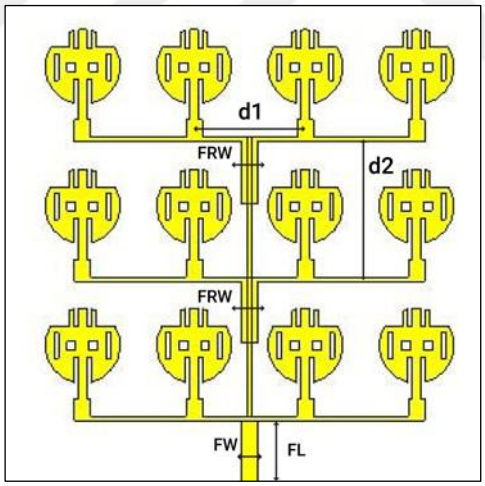

Figure 4.8: 3x4 Antenna Array Design.

in 2D design, the relation between the bandwidth and the gain should considered for the best requirements. For the image resolution of the reflected target, a broad bandwidth is essential, however for automotive radar, gain and directive pattern takes precedence. In this case, we prefer to raise the gain while maintaining the necessary bandwidth and directive filed. This can be achieved by adjustment (the width of the each excitation row)

in order to configure the impedance at the operation band required. In contrast to the single-row form, in which the side lobes effect occurs in a single plane, phi = 0 in the 1x4 configuration. In this 2D 3x4 design, the SLL will affect two planes, phi = 0^0 and 90^0. Figure 4.9 illustrate the H-filed at phi = 0^0 & 90^0 for both FRW =1.5 mm and 1.85 mm at 14.5 GHz.

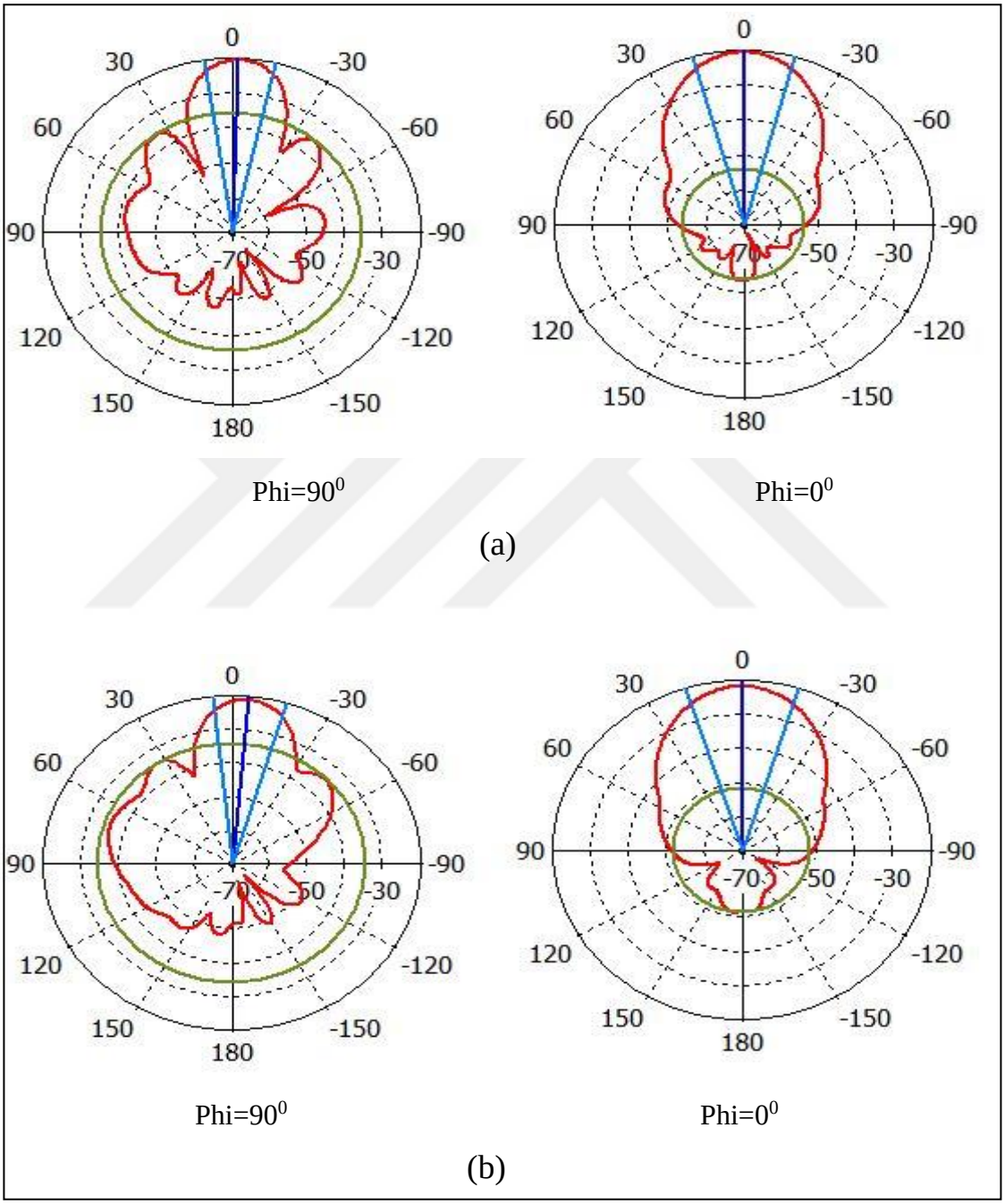

Figure 4.9: 3x4 Antenna Array H-Field At 14.5 Ghz (A) FRW=1.85 Mm (B) FRW=1.5 Mm.

As shown at plane Phi=0^0, the antenna obtain an extremely directional field and very low sidelobe level -30 dB in (a) design and -29 dB in (b) design. However, from the comparison between (a) and (b) H-field pattern we can recognized that at Phi=90^0 (a) is more directed. Figure 4.10 displays the relationship between the gain and the bandwidth. At FRW=1.85 mm, the gain achieved is 16.2 dBi at the center frequency, and this gain is maintained higher across the entire impedance bandwidth, making the curve more favorable than the one obtained with FRW=1.5 mm. Nevertheless, the bandwidth at FRW=1,85 mm was wider where the BW 821 MHz with S11 –29 dB and 400 MHz with S11 –34 dB at FRW=1.5 mm as depicted in Figure 4.11. overall, in V2X, its depends on the application. When it's come to radar, the directed field and high gain is preferred with suitable BW. while in Satellite, high gain and wider BW would be preferred.

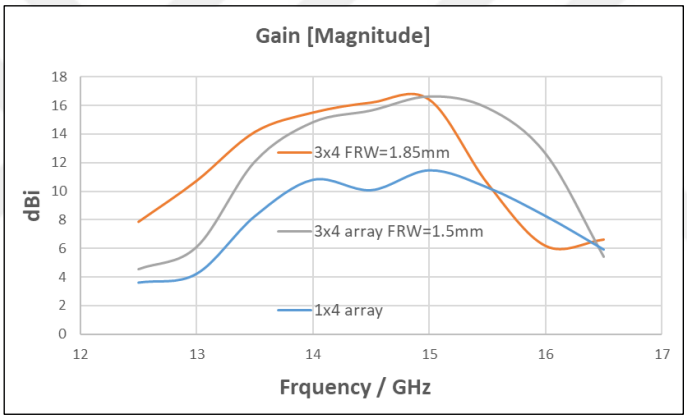

Figure 4.10: Antenna Arrays Gain.

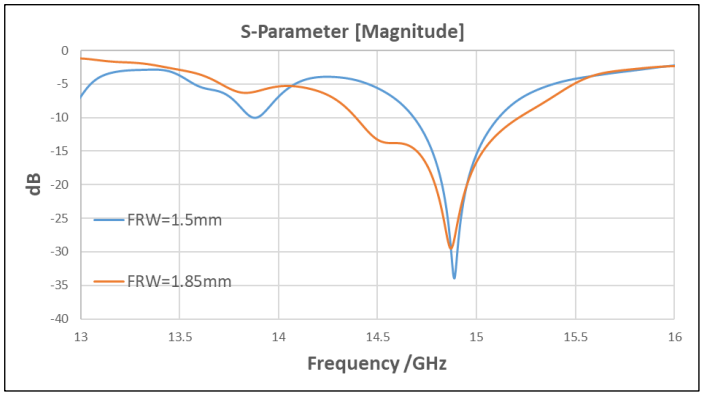

Figure 4.11: 3x4 Antenna Array Reflection Coefficient (S11).

Table 4.3, depicted briefly the metrics improvement over the single, 1x4 and 3x4 antennas. The SLL was the significate improvement in 3x4 array in addition to the gain. While 1x4 design have the best bandwidth achievement.

Table 4.3: Antennas Array Simulated Metrics Comparison.

Parameter	**Gain**	**Directivity**	**S11**	**Rad.Efficiency**	**Sidelobe level**	**Bandwidth**
Single/element (Novel)	7 dBi	7.98 dBi	–49 dB	76%	–14.1 dB phi=90^0	285 MHz
1x4 Array deign	11.3 dBi	12 dBi	–37 dB	86%	–21.3 dB	422 MHz
3X4 Array design	16.2 dBi	16.8 dBi	–29 dB	86%	–30 dB Phi=0^0 –15.1 dB Phi=90^0	821 MHz

5. FBRICATION AND RESULTS

5.1 ANTENNA FABRICATION

We have developed and simulate three different antenna prototypes. Prototypes of the proposed antennas have been fabricated in Altınbaş university laboratory. Figure 5.1 is a photograph of the fabricated antennas. The fabricated antennas are connected using SMA connectors at 50 Ohm, and their tiny size and low profile allow them to be placed on the majority of trade-off antenna transceivers. The antenna array's physical dimensions for single element, 1x4 array and 3x4 array are 18 mm x15 mm, 50 mm x 25 mm, 60 mm x 60 mm respectively.

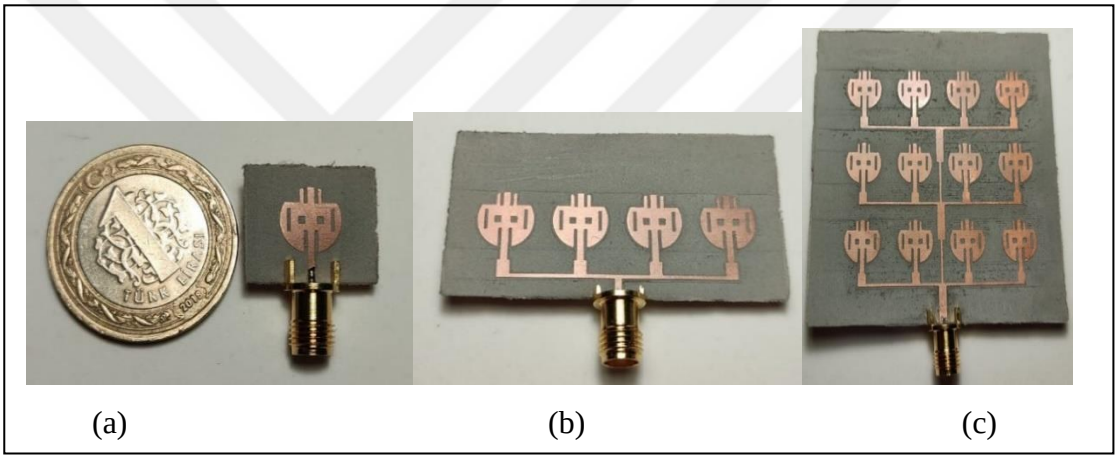

Figure 5.1: Fabricated Antennas (A) Single Element (B) 1x4 Antenna Array And (C) 3x4 Antenna Array.

5.2 LAB MEASUREMENTS

The antenna was constructed and measured using Rohde & Schwarz ZNB Vector Network Analyzer in RF Lab of Altınbaş university. The S11 parameter was tested. The dynamic range of the VNA permitted measuring frequencies ranging from 100MHz to 20GHz. Noting that all three manufactured antennas yielded nearly identical accuracy. Figure 5.2 Shows the S11 measuring of the three antennas.

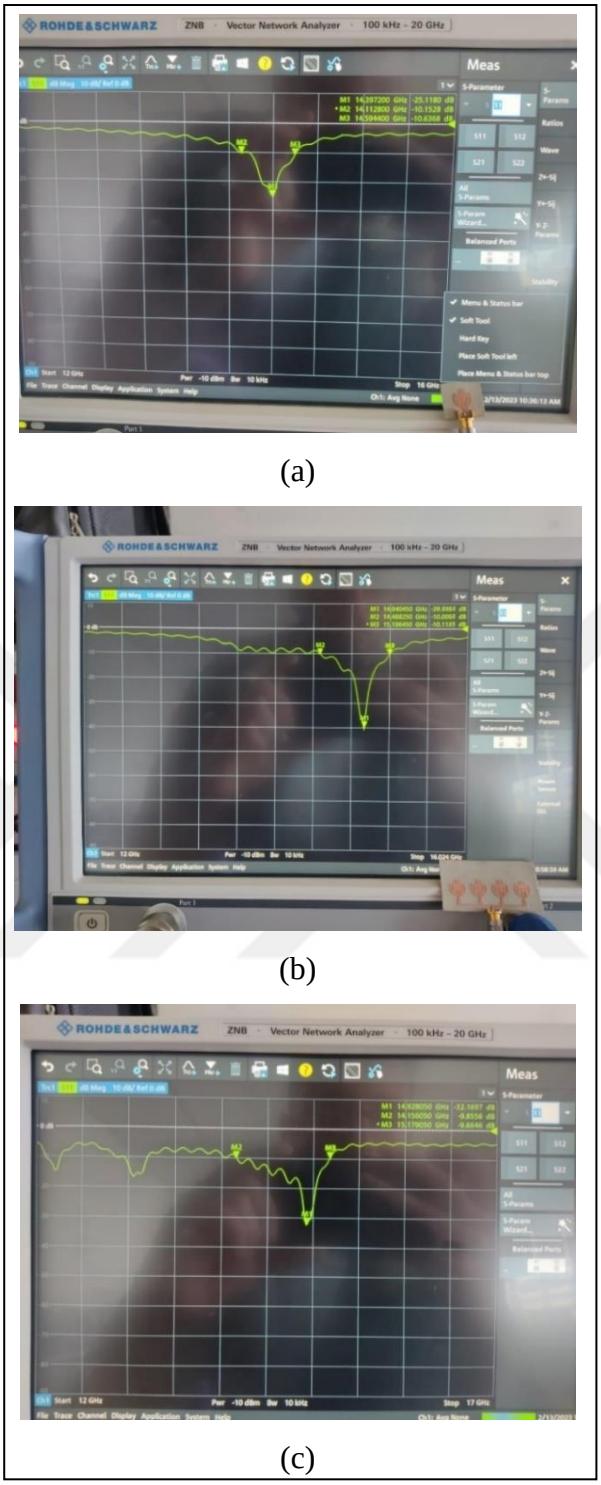

Figure 5.2: Lab Measurements S11 (A) Single Element, (B) 1x4 Array, (C) 3x4 Array.

Measurements taken in the Antennas Laboratory, shown in Figure 5.2 single element (a), one by four (b), and three by four (c) arrays. The S11 measurement from a single antenna element exceeded 400 MHz With a minimal S11 of -24.5 dB at 14.4 GHz and a bandwidth below –10 dB from 14.1 GHz to 14.6 GHz. The 1x4 array of antennas has obtained a –39.47 dB minimum S11 at 14.9 GHz and a bandwidth of 770 MHz between 14.43 GHz and 15.2 GHz. The minimum S11 of -32.16 dB was recorded at 14.9 GHz for the 3x4 antenna array S11 in frequency range 14.15–15.17 GHz, with a bandwidth of 1.02 GHz.

5.3 MEASURED RESULTS COMPARED WITH SIMULATED

One of the most important indicators is the bandwidth. The dielectric characteristics of a microstrip antenna are among the most influential factors in determining the bandwidth. A large frequency range may be achieved by employing a thick substrate and a high dielectric constant. While slotting approaches can't fully eliminate impedance losses, they can be adjusted somehow to improve BW. For this experiment, we used the Roger RT5880LZ lossy substrate since it has the lowest dielectric constant among commercially available substrates (2.0) and a relatively thin thickness (0.5mm). The bandwidth-limiting capabilities of this substrate type are exceptionally small. The slots not only helped regulate the impedance and achieve the optimal Reflection Coefficient, but from the fabrication results they also improved the bandwidth. The bandwidth improvements are depicted in Figure 5.3. As seen in 5.3a, the simulated bandwidth for the single-element antenna was 285 MHz, but the actual antenna's bandwidth was over 400 MHz. The 1x4 and 3x4 antennas have also been improved upon in the same way. In spite of the fact that the 1x4 and 3x4 simulated BW was near to 422 MHz, 821 MHz, the measured obtain 770 MHz, and 1.01 GHz, respectively, as shown in 5.3b and 5.3c.

Figure 5.3 shows how the slots' effect on measured antenna impedance over the operating band for single and array designs.

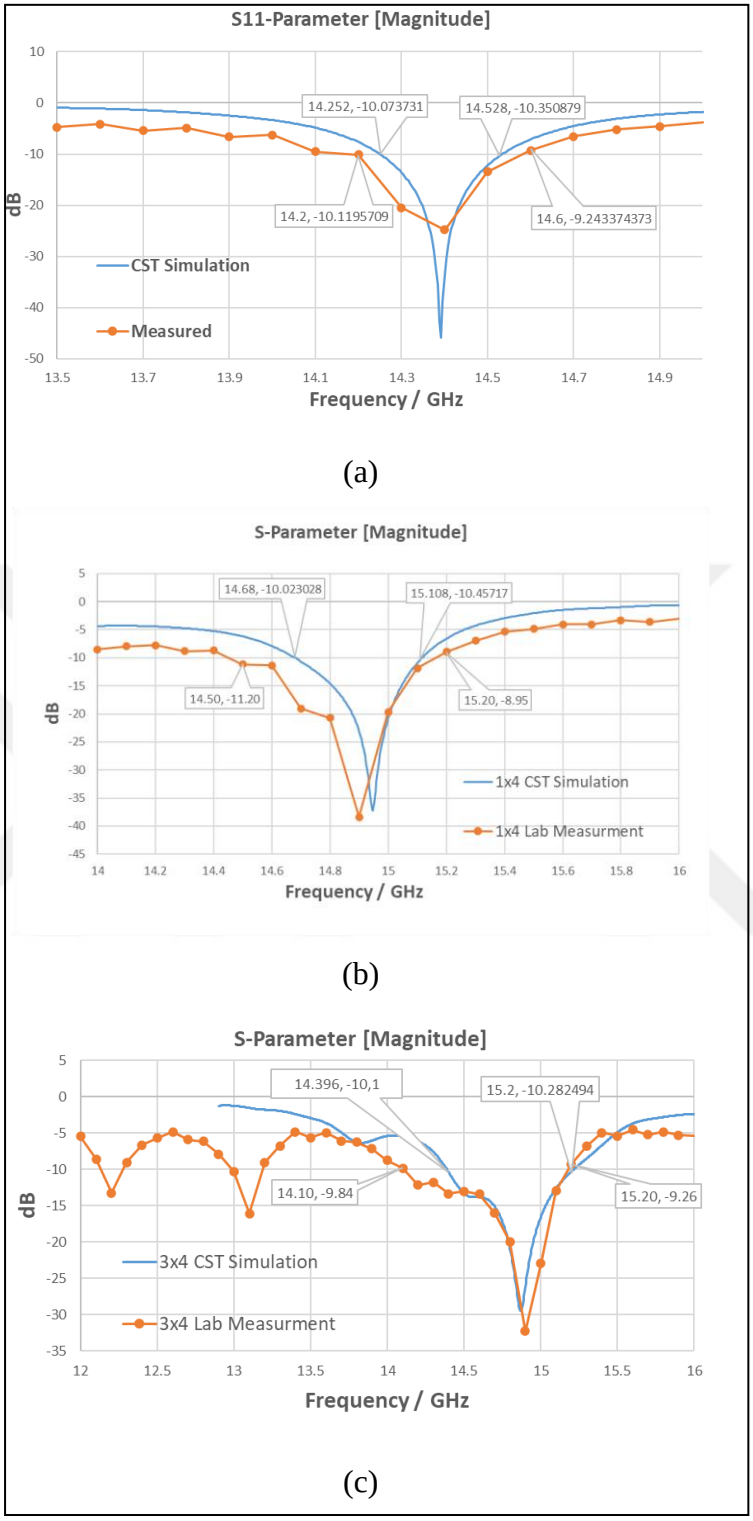

Figure 5.3: Simulated and Measured S11 (A) Single Element Antenna, (B) 1x4 Antenna Array And (C) 3x4 Antenna Array.

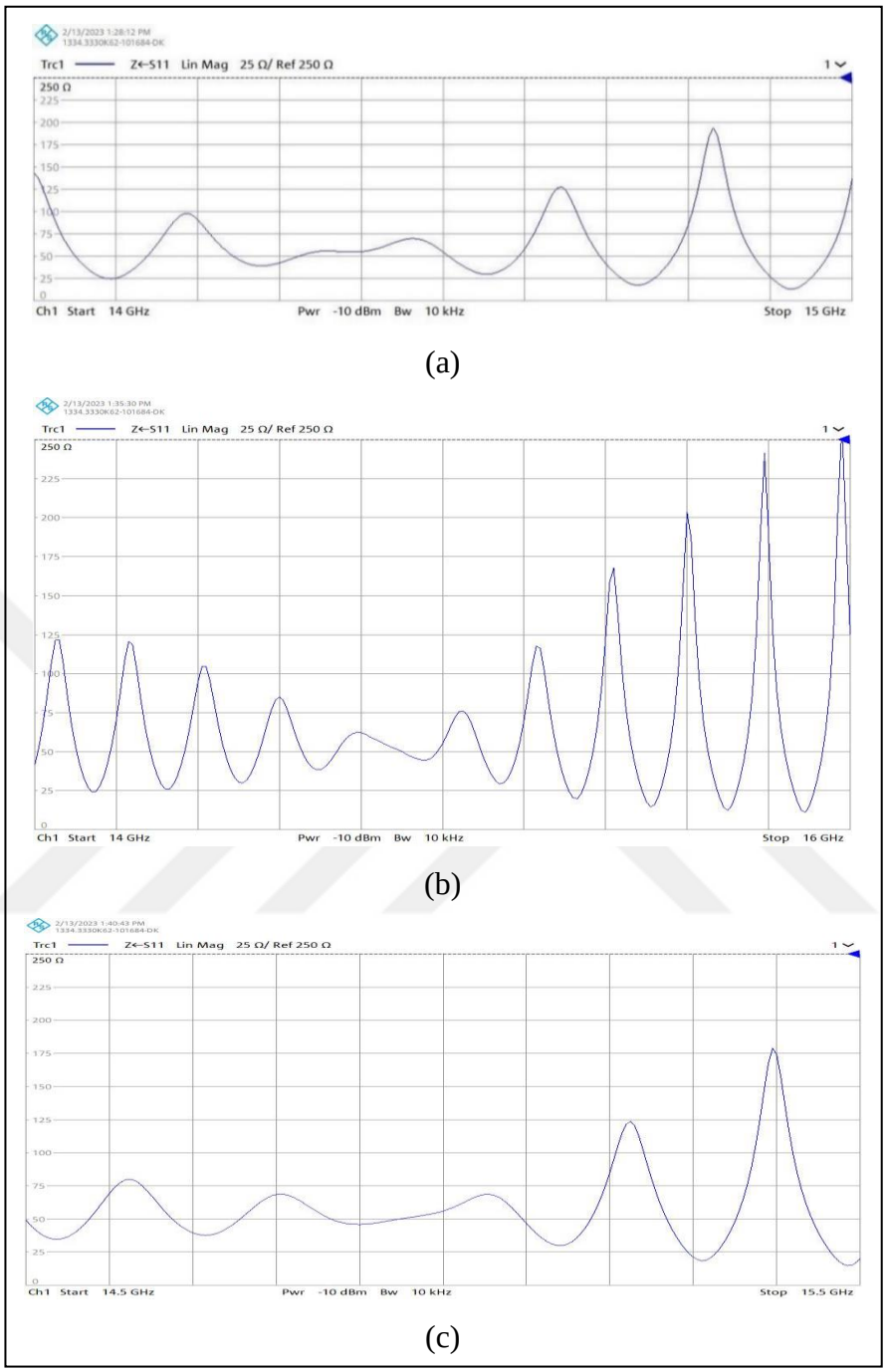

Figure 5.4: Measured Antennas Impedance (A) Single, (B) 1x4 Array, (C) 3x4 Array.

s

Table 5.1 below illustrate the antenna metrics comparation with the latest published related works.

Table 5.1: Antennas Array Simulated Metrics Comparison.

REF	Year	Sub high, ε	Element Num	BW GHz	Max Gain dBi	SLL dB	Efficiency %
[30]	2022	0.5mm, 3.6	8X8	23.7-24.6	24	-14	_
[30]	2022	0.25mm, 2.2	8X8	23.7-24.5	25	-24.5	_
[31]	2022	1.6mm, 3.0	Grid (31 segments)	17.3-17.8 14.14.5	10.4	_	84%
[41]	2019	0.25mm, 3.6	6X8	24-24.25	20.5	-19, -18	_
[33]	2017	0.25mm, 3.0	10X8	75.5-78	18.8	-16	_
[36]	2019	0.25mm, 3.6	8X12	23.5-24.5	22.26	-20.9	_
[37]	2017	0.25mm, 2.2	10X6	75-80	19	-15, -12	66%
This work	2023	0.5mm, 2.0	3X4	14.1-15.2	16.2	-30	86%

6. CONCLUSION AND FUTURE WORK

6.1 CONCLUSION

In this work, three modules of microstrip antennas for Ku band automobile applications are presented. for the first design of the single element which addressed in chapter 3, and in comparison, to standard microstrip patch antenna. The antenna offered use etching-loaded technology to improve Reflection Coefficient and gain. The functioning principle of the slotted-circular patch antenna is illustrated, as well as design formulations are given. at the beginning, As is common knowledge, the standard circular patch resonant frequency is dependent on a single parameter, the radius. The first contribution of employing the circular patch derived from the other shapes was to employ the etching technique to generate an additional dimensional parameter with the capability of controlling impedance.
The slotted circular patch simulated and measured Reflection Coefficient –49 dB, 24.5 dB respectively. The peak gain reach to 7 dBi. the overall size of the substrate 15x18 mm. with considering the substrate selection of the lower dielectric constant of 2.0 and very thin substrate thickness of 0.5 mm, The antenna obtain a good efficiency of 79% through 285 MHz simulated and 400 MHz measured bandwidth.
Then, 1D dimensional antenna array have designed and simulate dependent on the single element. 1x4 array have achieved a significant improvement in bandwidth. The simulated and measured S11 –37 dB, –39 dB at 14.9 GHz frequency with 770 MHz bandwidth and high peak gain of 11.3 dBi. Moreover, the E-field and H-field has shown the directed pattern and the low sidelobe level obtain –21 dB in both (E&H) plane. In addition, using the minimum feeding network decreases the unwanted radiation from the feed lines which in some cases increase the sidelobe level.
As mentioned before, the low selection of the dielectric constant helps in drop the power loss and enhance the performance of the antenna even with very thin thickness of the substrate. 1x4 antenna have obtain 87% and 86% as radiated and total efficiencies, respectively.
For more directivity and gain enhancement, 3x4 antenna have designed and simulated. While 2D designs produce the SLL effect in each phi=0^0 and 90^0. The antenna achieved very low sidelobe level reach to -30 dB at phi=0^0 in both E-plane and H-plane. In addition,

the gain has taken a significant improvement from 11.3 dBi in1x4 design to 16.2 dBi 3x4 design.

6.2 FUTURE WORK

There are numerous types of antenna array feeding networks. For automobile radar, series-feed is the most effective transmission method. However, as previously explained, series feeds occur in two forms (in line series connect and Shunt-series connection). In line series connections have the best minimization for the feeding network, resulting in highly compressed undesired radiation from the feeding network, which increases the level of sidelobes. in addition, the in line series connection provide the best antenna size reduction.

This type of feeding is utilized in numerous rectangular patch designs. Due to the rectangular shape, it is possible to adjust the needed impedance at each element by varying the width while retaining the length responsible for the resonant frequency.

In conventional circular patch, this technique cannot handle because of the circular patch have only one dimension responsible for the resonant frequency. This technique is incapable of handling standard circular patches due to the fact that circular patches only have a single dimension that is responsible for the resonant frequency.

In this thesis, the answer has been addressed by introducing a new dimensional parameter into the novel single-element design. By adjusting this value to tune the impedance of each element, a circular patch might be designed and tested with (in line series connection) while maintaining the same radius for all array elements. furthermore, one of the benefits of circular patches over rectangular ones is that they occupy a smaller substrate area.

REFERENCES

[1] P. Kaniewski, C. Lesnik, W. Susek, and P. Serafin, "Airborne radar terrain imaging system*," 6th International Radar Symposium (IRS)*, Dresden, Germany, 2015, pp. 248–253, 2015.

[2] M. Pachiyaannan and G. K. D. P. Venkatesan, "Dual-Band UWB Antenna for Radar Applications: Design and Analysis," *8th International Conference on Computational Intelligence and Communication Networks (CICN)*, Tehri, India, 2016, pp. 196–199.

[3] M. Kyriakidis, C. van de Weijer, B. van Arem, and R. Happee, "The Deployment of Advanced Driver Assistance Systems in Europe," *22nd ITS World Congress Bordeaux France. Available at SSRN 2559034*, 2015.

[4] J. Hasch, E. Topak, R. Schnabel, T. Zwick, R. Weigel, and C. Waldschmidt, "Millimeter-Wave Technology for Automotive Radar Sensors in the 77 GHz Frequency Band," *IEEE Transactions on Microwave Theory and Techniques*, vol. 60, no. 3, 2012, pp. 845–860.

[5] F. Roos, S. Member, D. Kellner, J. Dickmann, C. Waldschmidt, and S. Member, "Reliable Orientation Estimation of Vehicles in High-Resolution Radar Images," *IEEE Transactions on Microwave Theory and Techniques*, vol. 64, no. 9, 2016, pp. 2986–2993.

[6] A. Design, "Development of a mid-range automotive radar sensor for future driver assistance systems," *International Journal of Microwave and Wireless Technologies*, vol. 5, no. 1, 2013, pp. 15–23.

[7] *Radar handbook*, 3rd ed., McGraw-Hill Education, NC, 2008.

[8] Rabinovich, Victor, and Nikolai Alexandrov. Antenna arrays and automotive applications. ringer Science & Business Media, 2012.

[9] C. A. Balanis, Antenna Theory: Analysis and Design, 3rd Edition. 2005.

[10] *Modern antenna handbook*, Constantine A., ed, John Wiley & Sons, 2011.

[11] Y. Wang et al., "A 260-mW Ku-Band FMCW Transceiver for Synthetic Aperture Radar Sensor With 1 . 48-GHz Bandwidth in 65-nm CMOS Technology," *IEEE Transactions On Microwave Theory And Techniques*, vol. 65, no. 11, 2017, pp. 4385–4399.

[12] H. Sook, N. Joe, S. Yun, J. M. Kim, and S. Jeon, “Microstrip Patch Array Antenna with High Gain and Wideband for TdRx Dual Operation at Ku-Band,” *IEEE Antennas and Propagation Society Symposium,* Monterey, CA, USA, 2004. pp. 1–4.

[13] Xue, Fei, et al. "A broadband KU-band microstrip reflect array antenna using single-layer fractal elements." *Microwave and Optical Technology Letters,* 2016, pp. 658-662, 2016

[14] P. Subbulakshmi, “Rectangular Microstrip Patch Array Antenna,” *IEEE International Conference ON Emerging Trends in Computing, Communication and Nanotechnology (ICECCN),* Tirunelveli, India, 2013, pp. 547–552.

[15] N. M. Nor, M. H. Jamaluddin, M. R. Kamarudin, and M. Khalily, “Rectangular Dielectric Resonator Antenna Array for 28 GHz Applications,” *Progress In Electromagnetics Research*, 2016, vol. 63, no. April, pp. 53–61.

[16] Jamali and T. Cook, "Comparative study of microstrip patch antenna feed network," *International Conference on Radar*, Adelaide, SA, Australia, 2013, pp. 179-183.

[17] J. R. Panda and R. S. Kshetrimayum, “An Inset-fed Dual-Frequency Circular Microstrip Antenna with a Rectangular Slot for Application in Wireless Communication,” *International Conference on Emerging Trends in Electrical and Computer Technology*, Nagercoil, India, 2011, pp. 976–981.

[18] Z. Rahman, K. Chandra, D. Nath, and M. Mynuddin, “Performance Analysis of an Inset-Fed Circular Microstrip Patch Antenna Using Different Substrates by Varying Notch Width for Wireless Communications,” *International Journal of Electromagnetics and Applications*, no. November, 2020, pp. 19–29.

[19] S. B. Patil, R. D. Kanphade and V. V. Ratnaparkhi, "Design and performance analysis of inset feed microstrip square patch antenna for 2.4GHz wireless applications," *2nd International Conference on Electronics and Communication Systems (ICECS)*, Coimbatore, India, 2015, pp. 1194-1200.

[20] P. Kuravatti, “Comparison of Different Parameters of the Edge Feed and the Inset Feed Patch Antenna,” *International Journal of Applied Engineering Research*, vol. 13, no. 13, pp. 11285–11288, 2018.

[21] M. Singh, A. Basu and S. K. Koul, "Circular Patch Antenna with Quarter Wave Transformer Feed for Wireless Communication," *Annual IEEE India Conference*, New Delhi, Indi, 2006, pp. 1-5.

[22] M. V. Mokal, P. S. R. Gagare, and R. P. Labade, “Analysis of Micro strip patch Antenna Using Coaxial feed and Micro strip line feed for Wireless Application,” *IOSR Journal of Electronics and Communication Engineering (IOSR-JECE)*, 2017, vol. 12, no. 3, pp. 36–41, 2017.

[23] B. Abdennaceur and A. Badri, “Design and Optimization of Aperture Coupled Microstrip Patch Antenna Using Genetic,” *International Journal of Innovative Research in Science,*

Engineering and Technology, 2014, Vol. 3, Issue 5, pp. 12687–12694.

[24] Madhusudhana K, S Jagadeesha, Amith K Jain, “Proximity Coupled Micro-Strip Antenna for Bluetooth Application,” *International Journal for Research in Applied Science & Engineering Technology (IJRASET)*, 2019, Vol. 7, Issue VIII, pp. 234–237.

[25] N. Kaur and S. Malhotra, "A review on significance of design parameters of microstrip patch antennas," *5th International Conference on Wireless Networks and Embedded Systems (WECON)*, Rajpura, India, 2016, pp. 1-6.

[26] Y. I. Chong and D. Wenbin, "Microstrip series fed antenna array for millimeter wave automotive radar applications," *IEEE MTT-S International Microwave Workshop Series on Millimeter Wave Wireless Technology and Applications*, Nanjing, China, 2012, pp. 1-3.

[27] A. M. Zobu, B. Dağdeviren, G. Demirbaü, B. C. Kocaoğlu and E. Gürhan, "Low Sidelobe Level Antenna Array with Amplitude Tapering," *Microwave Mediterranean Symposium (MMS)*, Pizzo Calabro, Italy, 2022, pp. 1-4.

[28] C. Waldschmidt, J. Hasch and W. Menzel, "Automotive Radar — From First Efforts to Future Systems," *IEEE Journal of Microwaves*, 2021, vol. 1, no. 1, pp. 135-148.

[29] K. K. Naik and P. A. V. Sri, “Design of Hexadecagon Circular Patch Antenna with DGS at Ku Band for Satellite Communications,” *Progress In Electromagnetics Research M*, 2017, vol. 63, pp. 163–173, 2018.

[30] J. Shan, K. Rambabu, Y. Zhang, and J. Lin, “High gain array antenna for 24 GHz FMCW automotive radars,” *International Journal of Electronics and Communications*, 2021, vol. 147, pp. 154144, 2022.

[31] S. Arumugam, S. K. Palaniswamy, and S. Manoharan, “International Journal of Electronics and Communications High gain wide band grid array antenna for short range radar and vehicle-to-satellite communications,” *International Journal of Electronics and Communications*, 2021, vol. 147, p. 154157, 2022.

[32] Zhang, X. M., et al. "Stacked series-fed linear array antenna with reduced sidelobe." *Electronics Letters*, 2014, Vol. 50 No. 4, pp. 251–253.

[33] J. Xu, W. Hong, H. Zhang, and Y. Yu, “Design and measurement of array antennas for 77GHz automotive radar application,” *10th UK-Europe-China Workshop on Millimeters Waves and Terahertz Technologies (UCMMT)*, Liverpool, UK, 2017, pp. 1-4.

[34] N. Boskovic, B. Jokanovic, M. Radovanovic, and N. S. Doncov, “Novel Ku-Band Series-Fed Patch Antenna Array with Enhanced Impedance and Radiation Bandwidth,” *IEEE Transactions On Antennas And Propagation*, 2018, vol. 66, no. 12, pp. 7041–7048.

[35] I. Slomian, K. Wincza, and S. Gruszczynski, “Low-cost broadband microstrip antenna array for 24 GHz FMCW radar applications,” *International Journal of RF and Microwave Computer-Aided Engineering*, 2013, vol. 23, no. 4, pp. 499–506.

[36] Y. Jia, Y. Liu, and Y. Zhang, “A 24 GHz microstrip antenna array with large space and narrow beamwidth,” *Microwave and Optical Technology Letters*, 2020, vol. 62, no. 4, pp. 1615–1620.

[37] M. G. Automotive, “An Array Antenna for Both Long- and Radar Applications,” *Ieee Transactions On Antennas And Propagation*, 2017, vol. 65, no. 12, pp. 7207–7216.

[38] S. B. Yeap, X. Qing, and Z. N. Chen, “77-GHz Dual-Layer Transmit-Array for Automotive Radar Applications,” *IEEE Transactions on Antennas and Propagation*, 2015, Vol. 63, Issue. 6, pp. 1–5.

[39] J. Xu, Z. N. Chen, and X. Qing, “CPW Center-Fed Single-Layer SIW Slot Antenna,” *IEEE Transactions On Antennas And Propagation*, 2014, vol. 62, no. 9, pp. 4528–4536, 2014.

[40] K. Lomakin et al., “3D Printed Slotted Waveguide Array Antenna for Automotive Radar Applications in W-Band,” *48th European Microwave Conference (EuMC)*, Madrid, Spain, 2018, pp. 1409–1412.

[41] Y. Chen, Y. Liu, Y. Zhang, Z. Yue and Y. Jia, "A 24GHz Millimeter Wave Microstrip Antenna Array for Automotive Radar," *International Symposium on Antennas and Propagation (ISAP)*, Xi'an, China, 2019, pp. 1-2.

[42] A. A. Roy, J. M. Môm and D. T. Kureve, "Effect of dielectric constant on the design of rectangular microstrip antenna," *IEEE International Conference on Emerging & Sustainable Technologies for Power & ICT in a Developing Society (NIGERCON)*, Owerri, Nigeria , 2013, Vol. 21, Issue. 1, pp. 111-115.

[43] E. S. GÜLER, F. C. Gülin. "Material selection for microstrip antenna using critic-miacra integration as a practical approach*." Eskişehir Technical University Journal of Science and Technology A-Applied Sciences and Engineering*, 2020, pp. 1-20.

[44] M. A. H. Oweis and H. H. M. Ghouz, “A novel Ku-band microstrip antenna*,” International Conference on Engineering and Technology (ICET)*, Cairo, Egypt, 2015, pp. 1–4.

[45] Y. Rhazi, I. Journal, Y. Rhazi, S. Bri, R. Touahni, and S. Faculty, “The Effect of the Radius of the Circular Patch Antenna in the Ku-Band,” *International Journal of Microwaves Applications*, 2014, vol. 3, no. 6, pp. 35–37.

[46] K. K. Naik and P. A. V. Sri, “Design of Hexadecagon Circular Patch Antenna with DGS at Ku Band for Satellite Communications,” *Progress In Electromagnetics Research M*, 2018, vol. 63, pp. 163–173, 2018.

[47] F. Foysal, S. Mahmud, and A. K. M. Baki, “A Novel and High Gain Antenna Design for Autonomous Vehicles of 6G Wireless Systems,” *International Conference on Green Energy, Computing and Sustainable Technology (GECOST)*, Miri, Malaysia, 2021, pp. 1–5.

[48] N. H. M. Adnan, I. M. Rafiqul, and A. H. M. Zahirul Alam, “Effects of inter element spacing on large antenna array characteristics,” *IEEE 4th International Conference on Smart Instrumentation, Measurement and Application (ICSIMA)*, Putrajaya, Malaysia, 2018, pp. 1–5

[49] Y. Konishi, “Phased array antennas*,” IEICE Transactions On Communications*, 2003, vol. E86-B, no. 3, pp. 954–967.

[50] A. Aydemir, “Development of K Band Microstrip Patch Antenna Array for Traffic Radar,” M.Sc.Thesis, ECE Eng, Middle East Univ, Turkiye. November, 2017.